KfK 4349
Februar 1988

Intercomparison of Transmittance and Radiance Algorithms (ITRA)

Report of the Limb-Group of the ITRA-Workshop at the University of Maryland 12 - 14 March 1986

H. Fischer, G. P. Anderson, T. v. Clarmann, S. A. Clough,
M. T. Coffey, A. Goldman, F. X. Kneizys
Institut für Meteorologie und Klimaforschung
AFGL, Air Force Geophysics Laboratory
NCAR, National Center of Atmospheric Research
University of Denver

Kernforschungszentrum Karlsruhe

KERNFORSCHUNGSZENTRUM KARLSRUHE

Institut für Meteorologie und Klimaforschung

KfK 4349

Intercomparison of Transmittance and Radiance Algorithms (ITRA)

Report of the Limb – Group of the ITRA – Workshop

at the University of Maryland

12 – 14 March 1986

H. Fischer, G.P. Anderson[1], T.v. Clarmann, S.A. Clough[1],

M.T. Coffey[2], A. Goldman[3] and F.X. Kneizys[1]

Kernforschungszentrum Karlsruhe GmbH, Karlsruhe

[1] AFGL, Air Force Geophysics Laboratory

[2] NCAR, National Center of Atmospheric Research

[3] University of Denver

Kernforschungszentrum Karlsruhe GmbH
Postfach 3640, 7500 Karlsruhe 1

ISSN 0303-4003

ABSTRACT

An Intercomparison of Transmittance and Radiance Algorithms (ITRA) Workshop took place at the University of Maryland in March 1986. The limb subgroup participants compared the results of their different line-by-line computer codes which were applied on various limb sounding cases. Frequently, the calculated spectra and integral values agreed very well. But, in some cases considerable discrepancies have been identified which are due to:

- the applied line shape functions
- the special assumptions on line wings
- the consideration of lines outside the given spectral interval
- the handling of the spectral sampling function

When identical spectroscopic constraints were provided, including line shape and procedures for defining line cutoff, the agreement of the results was improved significantly.

ZUSAMMENFASSUNG

Bericht der Arbeitsgruppe Horizontsondierung der ITRA – Arbeitstagung an der Universität von Maryland vom 12. bis 14. März 1986

Im März 1986 fand an der Universität von Maryland ein IRC (International Radiation Commission) – Workshop statt, der den Vergleich von Transmissions und Strahldichtealgorithmen zum Thema hatte. Die Teilnehmer der Arbeitsgruppe 'Horizontsondierung' verglichen die Ergebnisse ihrer verschiedenen Linie – für – Linie Rechenprogramme für diverse Horizontsondierungsgeometrien und unterschiedliche Spektralbereiche. Häufig stimmten die berechneten Spektren und integralen Werte gut überein. In einigen Fällen traten jedoch beträchtliche Abweichungen auf, die auf folgende Ursachen zurückzuführen sind:

- unterschiedliche Formfunktionen der Spektrallinien

- unterschiedliche Annahmen über die Linienflügel

- unterschiedliche Berücksichtigung der Flügel der Linien außerhalb des zugrundegelegten Spektralintervalls

- die Handhabung der Gerätefunktion

Eine teilweise Vereinheitlichung der spektroskopischen Parameter, insbesondere in bezug auf die Formfunktion der Linien und die Berücksichtigung der Linienflügel, führte zu einer erheblich verbesserten Übereinstimmung der Ergebnisse.

PARTICIPANTS

of the ITRA – Limb – Subgroup

AFGL:	S.A. Clough
	G.P. Anderson
	F.X. Kneizys
DU:	A. Goldman
MIM:	H. Fischer, Chairman
	(current address: Kernforschungszentrum Karlsruhe, IMK)
	T.v. Clarmann
	(current address: Kernforschungszentrum Karlsruhe, IMK)
NCAR:	M.T. Coffey
Observers:	L.S. Rothman, AFGL
	L. Gordley, NASA Langley
	V. Kunde, GSFC

AFGL:	Air Force Geophysics Laboratory
DU:	Denver University
MIM:	Meteorologisches Institut der Universität München
NCAR:	National Center of Atmospheric Research
GSFC:	Goddard Space Flight Center

For complete addresses, see Appendix E

CONTENTS

1. INTRODUCTION

In 1981 the International Radiation Commission (IRC) established a Working Group on Remote Sensing with the order to:

- compile all available information on spectral transmission functions and computation procedures in those spectral regions which are of importance for remote sensing,
- select well-documented spectral measurements against which computed transmittances and radiances can be compared, and
- organize an international comparison of transmittance and radiance computation algorithms based upon a pilot data set in order to determine the accuracy which can be achieved with the different calculation methods.

The first activity of this WG resulted in a comparison of line-by-line calculations with laboratory spectra of the 15 μm CO_2 band. The findings have been summarized in an unpublished report by A. Chedin (Jan., 1984).

In 1982 the IRC initiated through its Remote Sensing WG an Intercomparison of Transmittance and Radiance Algorithms (ITRA, chairman A. Chedin) appropriate for atmospheric conditions. Three subgroups were established for this exercise: Nadir subgroup (chairman D. Spänkuch), limb subgroup (chairman H. Fischer) and microwave subgroup (chairman K. Künzi). The members of the WG agreed to perform calculations of spectral transmittances and radiances for some model atmospheres and for selected spectral intervals. The results of these calculations were discussed at the ITRA Workshop at the University of Maryland in College Park, Maryland, March 12-14, 1986. This workshop was organized by A. Arking (NASA, GSFC) and A. Chedin (LMD, CNRS). About 30 participants contributed to the success of the ITRA Workshop.

The following report covers the findings of the limb subgroup. Similar reports have been prepared by the nadir and the microwave subgroups.

The nadir subgroup report contains a description of the basic formulas of line-by-line computer codes. Also, the causes of discrepancies between the results of different codes are mentioned. Readers without sufficient background of this research area are referred to the nadir subgroup report.

2. DEFINITION OF THE EXERCISE

The participating scientists were provided with detailed information to carry out the exercise:

Exercise 1: This exercise was prepared in advance of the ITRA meeting at the University of Maryland, 12 – 14 March 1986. The spectroscopy (line wings, continuum, temperature dependence of line half width etc.) was not defined in detail due to the differences in the structure of the computer codes used. But it was expected that each participant of the exercise specify the spectroscopic conditions assumed in his calculations.

To avoid inconsistencies in the results of the time consuming line – by – line calculations arising solely from the atmospheric layering algorithm, the participants were provided with mean layer values $\bar{p}_i$, $\overline{T_i}$ and the column amounts u_i of the layers for selected slant paths (see App. A). In addition, participants were to use their own algorithms to calculate $\bar{p}_i$, $\overline{T_i}$ and u_i in order to compare with the given values.

The conditions for the first exercise of the limb subgroup were:

1. Spectral regions

1.1. 15μm

Absorber: only CO_2

Spectral Intervals:

a) 685 – 695 cm^{-1}

b) 715 – 725 cm^{-1}

c) 732 – 764 cm^{-1}

The last spectral interval is identical with one of the nadir subgroup (HIRS – channel 7)

1.2 6.3 μm

Absorber: H_2O and NO_2 (without O_2 and CH_4 absorption)

Spectral interval:

1600 – 1610 cm^{-1}

2. Conditions for the line - by - line calculations

2.1. Basis of line parameters

AFGL 1982

2.2 Filter functions for integral radiance values

triangular

Central wave number (cm^{-1})	Half - power band width (cm^{-1})
690	5
720	5
748	16
1605	5

2.3. Transmittance and radiance spectra

Spectral intervals as defined in section 1

spectral resolution: 0.05 cm^{-1} (half power band width)

triangular instrumental function

2.4. Line profile

Voigt line profile in principle

For CO_2 Sub - Lorentzian line wings recommended

Cut - off of the line wings should be indicated

3. Atmospheric models

3.1. Basic parameters

Three different models (see App. A)

- isothermal hydrostatic atmosphere T = 250 K
- isothermal hydrostatic atmosphere T = 296 K
- US Standard Atmosphere 1976

3.2 Concentration profiles

The mixing ratio profiles of the trace gases CO_2, H_2O and NO_2 are defined for pressure levels so that they can be used for all three atmospheres (see App. A).

3.3. Calculation of mean values $\bar{p}_i$, $\overline{T_i}$ and the column amounts u_i for the layers

The interpolation technique for determining sublayers is the following:

a) Select appropriate p levels

b) Temperature and trace gas mixing ratios are interpolated linearily with log p

The mean values $\bar{p}_i$, $\overline{T_i}$ have been calculated with the Curtis – Godson approximation after dividing the layers into several sublayers. Refraction effects have been taken into account.

4. Calculation of mass path for different tangent heights

The transmittance and radiance values calculated by the participants should not depend on the mean values for pressure $\bar{p}_i$ and temperature $\overline{T_i}$ and the column amounts u_i. Therefore, tables showing these values for all the cases were sent to each participant (see App. A).

In addition, any participant should calculate $\bar{p}_i$, $\overline{T_i}$ and u_i with his own subroutine in order to make comparisons. For this purpose the results have to be commented:

a) Interpolation technique for the generation of sublayers

b) Method for the determination of mean values $\bar{p}_i$, $\overline{T_i}$ and the column amounts u_i

c) Treatment of the first layer above the tangent height

d) Treatment of the refraction
For the lowest tangent height z_{Min} the calculation should be performed both considering refraction (z_{Min} = 10 km) and neglegting refraction (using the same observation angle so that z_{Min} > 10 km)

5. Definition of the spectral quantities to be calculated including formats

5.1. Calculation of spectral and integral transmittance values and radiances for three different slant pathes (z_{Min} = 10, 30, 50 km) and three different atmospheres as defined above

5.2 Presentation of the results

a) Tables of the integral transmittance values τ for the given atmospheric levels and integral radiances L at the top of the atmosphere

b) Plots of the spectral transmittance for all cases (degraded with the instrumental function as defined in section 2.3)

τ = 0.1 corresponds to 2 cm
$\Delta\nu$ = 1 cm^{-1} corresponds to 2 cm

c) Plots of the spectral radiance (degraded, see section 2.3) only for the Standard Atmosphere.
L should be normalized for reasonable comparisons:

$L' = L/L_{Max}$

L_{Max} is the maximum radiance in the spectral interval

$\Delta L'$ = 0.1 corresponds to 2 cm
$\Delta\nu$ = 1 cm^{-1} corresponds to 2 cm

d) Plots of the path weighting function for the integrated transmittance

For further comparisons plots of the normalized path weighting function $\Delta\tau/\Delta z$ are desired

Exercise 2: After having discussed the results of the participants during the ITRA - Workshop, a second exercise was defined to make possible further comparisons. In order to find out if some of the identified discrepancies are due to different spectroscopic assumptions, the participants agreed on the following:

1)
- All three CO_2 channels (see exercise 1)
- US Stand. Atm. and isothermal Atm. 296K
- Tangent heights: 30 km and 50 km
- Lorentzian line wings
- Contributions from spectral lines outside the defined spectral interval from ν_1 to ν_2: Calculations should include contributions from all lines from $\nu_1 - 25\ cm^{-1}$ to $\nu_2 + 25\ cm^{-1}$.
- Temperature dependence of halfwidth: exponent for CO_2: 0.75

2)
- H_2O channel
- US Standard Atmosphere
- Tangent height: 30 km
- Lorentzian line wings
- Contributions from spectral lines outside the defined spectral interval from ν_1 to ν_2: Calculations should include contributions from all lines from $\nu_1 - 25\ cm^{-1}$ to $\nu_2 + 25\ cm^{-1}$.
- Temperature dependence of halfwidth: exponent for H_2O and NO_2: 0.5

No ITRA2 10 km calculations have been performed, because the results of calculations at low tangent heights are strongly dependent on detailed spectroscopic assumptions. Such a comprehensive standardization of initial spectroscopic conditions in the computer codes would require severe changes of the algorithms in some cases.

3. MAIN DIFFERENCES BETWEEN THE LINE - BY - LINE COMPUTER CODES OF THE PARTICIPANTS

The participants used four different computer codes for generating the spectra and the integral transmittances and radiances. In the following some of the main differences between these codes are briefly described.

The AFGL - group (S.A. Clough et al.) used the widely known FASCOD2 program. The line wings can be modified by the χ - factor and are cut off at a distance of 25 cm^{-1} from the line center. Effects by the line wings beyond 25 cm^{-1} are simulated by precalculated continuum contributions.

The line - by - line code of M.T. Coffey and W.G. Mankin (NCAR) uses a transformation of the spectral lines into the Fourier space because the computation time is almost independant of the number of lines. On the other hand, the use of different line shapes is restricted, and lines outside the given spectral interval cannot be taken into account with this algorithm.

A. Goldman (University of Denver) used for his calculations a cut - off of the line wings at a distance of 5 cm^{-1} (ITRA1) and 25 cm^{-1} (ITRA2) from the line centers. The wings of lines outside the given spectral interval were taken into account within the same ranges.

The line - by - line code of the Meteorological Institute Munich (MIM, University of Munich) is mainly characterized by the consideration of all wings of available lines within and outside the given spectral interval which are contributing to the absorption coefficient at any mesh point within the given spectral interval. The selection of the contributing lines is done with a special criterion. The wings of the lines from outside are superimposed to form a quasi - continuum that depends on the given spectral interval.

More information about these four line - by - line computer codes is given in Appendix D.

4. COMPARISON OF THE RESULTS

In this report only results submitted until September 1986 are discussed. The amount of comparison is reduced because most of the participants did not calculate all the cases of the exercises (see Table 1).

There was no intercomparison of weighting functions, atmospheric refraction effects, or pressure and temperature mean values; only a few intercomparisons of the isothermal cases could be performed.

In most cases, the results agreed very well. Nevertheless, significant discrepancies could be recognized in some cases. Fig. 1 shows an example of discrepancies in transmittance in the gaps between the lines. Discrepancies are due to some characteristic features of the individual line-by-line computer codes:

- Peaks of the lines and gaps between the lines in the spectra are cut off and shifted by the sampling function
- Discrepancies at the gaps between the lines are caused by the use of different line shape functions and
- by the different handling of the wings of distant lines, as well as the continuum absorption

Discrepancies of the mass calculations do not influence the results of the transmittance and radiance calculations, because the participants calculated with the same absorber amounts. Nevertheless, the problem of absorber mass calculation shall be briefly discussed in this report.

Tab. 1: The participants calculated the following cases:

Case			AFGL		DU		NCAR		MIM			
Atmosphere	Tan.Ht.	Wavenumber	1	2	1	2	1	2	1	2		
Std. Atm.	50	685-695	x	x			x	x	x	x		
Std. Atm.	30	685-695	x	x		x	x	x	x	x		
Std. Atm.	10	685-695	x	x			x	x	x			
250 K	50	685-695							x			
250 K	30	685-695	x	x			x	x	x			
250 K	10	685-695							x			
296 K	50	685-695							x	x		
296 K	30	685-695	x	x				x	x	x		
296 K	10	685-695							x			
Std. Atm.	50	715-725	x				x	x	x	x		
Std. Atm.	30	715-725	x				x	x	x	x		
Std. Atm.	10	715-725	x				x	x	x			
250 K	50	715-725							x			
250 K	30	715-725	x	x				x	x			
250 K	10	715-725							x			
296 K	50	715-725							x	x		
296 K	30	715-725	x	x				x	x	x		
296 K	10	715-725							x			
Std. Atm.	50	732-764	x					x	x	x		
Std. Atm.	30	732-764	x					x	x	x		
Std. Atm.	10	732-764	x					x	x			
250 K	50	732-764							x			
250 K	30	732-764	x					x	x			
250 K	10	732-764							x			
296 K	50	732-764							x	x		
296 K	30	732-764	x					x	x	x		
296 K	10	732-764							x			
Std. Atm.	50	1600-1610	x	x	x		x		x	x		
Std. Atm.	30	1600-1610	x	x	x	x	x		x	x		
Std. Atm.	10	1600-1610	x	x	x		x		x			
250 K	50	1600-1610							x			
250 K	30	1600-1610	x						x			
250 K	10	1600-1610							x			
296 K	50	1600-1610							x	x		
296 K	30	1600-1610	x						x	x		
296 K	10	1600-1610							x			

Fig. 1: Example of the ITRA1 Exercise:
discrepancies in the gaps between the lines.
CO_2 – channel, 685 – 695 cm^{-1}, transmittance,
tangent height = 30 km

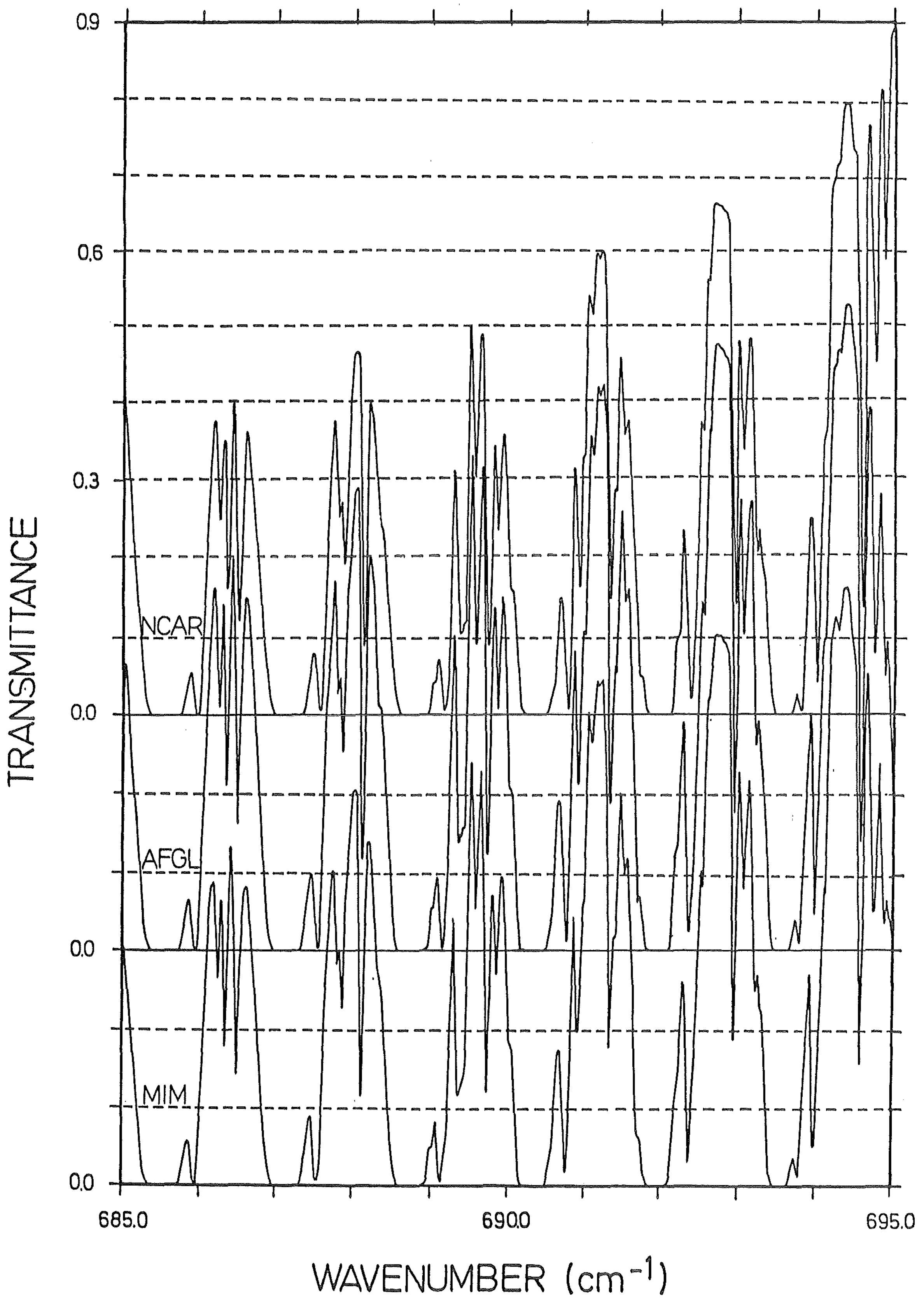

4.1 MASS CALCULATION

Tab. 2: Absorber amounts in the tangent path for z_{Min} = 30 km

	NCAR	AFGL	DU	MIM	greatest discrepancy
CO_2 US76Std	$6.59 \cdot 10^{21}$	$6.49 \cdot 10^{21}$	$6.55 \cdot 10^{21}$	$6.52 \cdot 10^{21}$	1.50%
CO_2 250 K isoth.	$9.49 \cdot 10^{21}$			$9.37 \cdot 10^{21}$	1.26%
H_2O US76Std	$8.80 \cdot 10^{19}$		$8.96 \cdot 10^{19}$	$8.91 \cdot 10^{19}$	1.79%
NO_2 US76Std	$1.298 \cdot 10^{17}$		$1.322 \cdot 10^{17}$	$1.316 \cdot 10^{17}$	1.81%

[The unit of the absorber amounts is molec./cm^2]

These are the values that would be calculated by the individual mass calculation subroutines; for the further calculations (transmittance and radiance) the ITRA - defined absorber amounts have been used.

The discrepancies of the calculated absorber amounts seem to be small, but some remarks must be made in this context.

The input parameter for these calculations is the tangent height, and not the observing angle and the observer height. Therefore, several errors that are due to incorrect geometrical calculations (handling of refraction, calculation of tangent height etc) are kept small. Also, no critical (i.e. non - uniformly mixed) gas profiles have been used. With different geometrical input values and different gases (e.g. CO or HNO_3) the discrepancies would probably be greater. Another reason, why discrepancies of absorber amounts were kept small in this exercise is that some of the participants used the given mean values $\bar{p}_i$ and $\overline{T}_i$ as input values instead of calculating there own ones for this special comparison.

For the following investigations the mass calculations have no influence on the agreement of the calculated spectra, because all the participants used the same absorber amounts as input parameter.

4.2 COMPARISON OF SPECTRA: SAMPLING FUNCTION

Spectral plots with a very high resolution do not allow comparisons with measurements. Thus, the very high resolution spectra are degraded by a sampling function (half width 0.1 cm^{-1}).

This sampling function may cause certain discrepancies in the extreme values of the spectrum (peaks of spectral lines, gaps between lines). (Fig. 2). Any sampling function will degrade the extreme values by averaging over a certain interval and will shift them, if the new mesh point of the sampling function is not identical to the mesh point of the extreme value. The sampling function of the ITRA exercise was defined as a triangular function. This kind of sampling function is very sensitive to the location of the peak of a line. If the peak of the triangle does not fit to the peak of a spectral line, the peak of the line will be reduced to a certain degree. Considering absolute values this means that peaks and gaps in the spectrum are less distinctive. If the absolute maximum radiance of the considered spectral range is used for normalization, and this absolute maximum is degraded by the sampling function, the sign and the size of the deviation depend on the dominance of either the cutoff effect or the normalization effect.

The disagreement of some ITRA1 results may be caused – among other differences between the algorithms, as different spectroscopic assumptions (e.g. line shape, continuum) – by sampling errors.

To avoid this kind of discrepancy, the participants of the workshop have done the calculations of the second exercise taking care to use appropriate sampling functions: Either a smoother, not much sensitive sampling function, like the Gauss – function has been used, or the step width of the function has been kept small.

Probably, the remaining discrepancies of the ITRA2 exercise cannot be ascribed to sampling errors.

Fig. 2: Example of discrepancies that may be caused by the sampling function; H_2O - channel; tangent height = 30 km

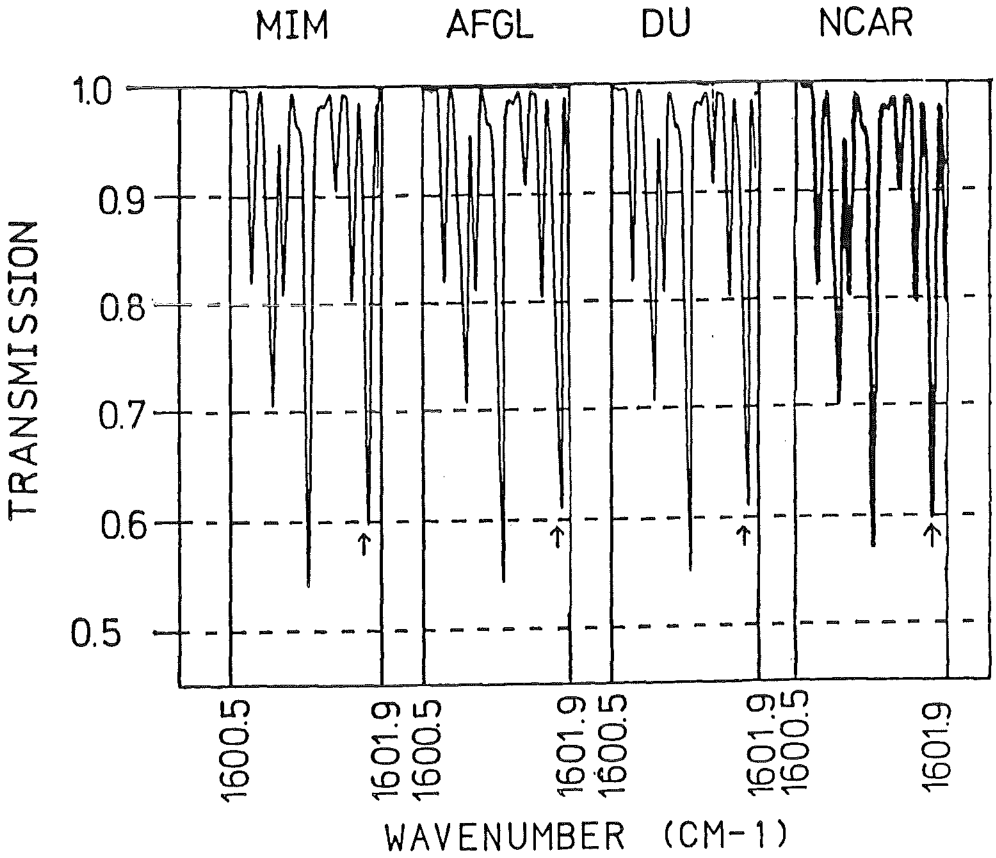

4.3 LINE SHAPE FUNCTION

Some of the discrepancies within the gaps between the lines are caused by the use of different line shape functions and temperature dependence of the line halfwidth. The reason for this was that the spectroscopic conditions were not defined in detail for the first limb subgroup exercise.

Fig. 3 shows results for CO_2 in the 685 – 695 cm^{-1} range. The calculations have been performed with the MIM code by using different line shape functions. Considerable deviations in transmittance can be recognized in the gaps between the lines.

The influence of a variable exponent n of the temperature dependence of the line halfwidth on spectral transmittance is shown in Fig. 4. In this part of the spectrum the change of the exponent results in a considerable change of transmittance which is of the same order or size as the difference between the curves in Fig. 3. It can be concluded that the selection of the right input parameters plays an important role at least for the generation of high resolution spectra.

Therefore, the participants of the limb subgroup agreed on the same line shape functions and the same exponent of the temperature dependence of the line halfwidth for the second exercise. Most of the discrepancies between the spectra could be considerably reduced (compare Fig. 1 to Fig 7, for instance).

Fig. 3: CO_2, transmittance, 685 - 695 cm^{-1}, tangent height = 30 km.

Both plots are created with the MIM - Program.

Run 1: Sub - Lorentzian line shape: - - -

Run 2: Lorentzian line shape: ————

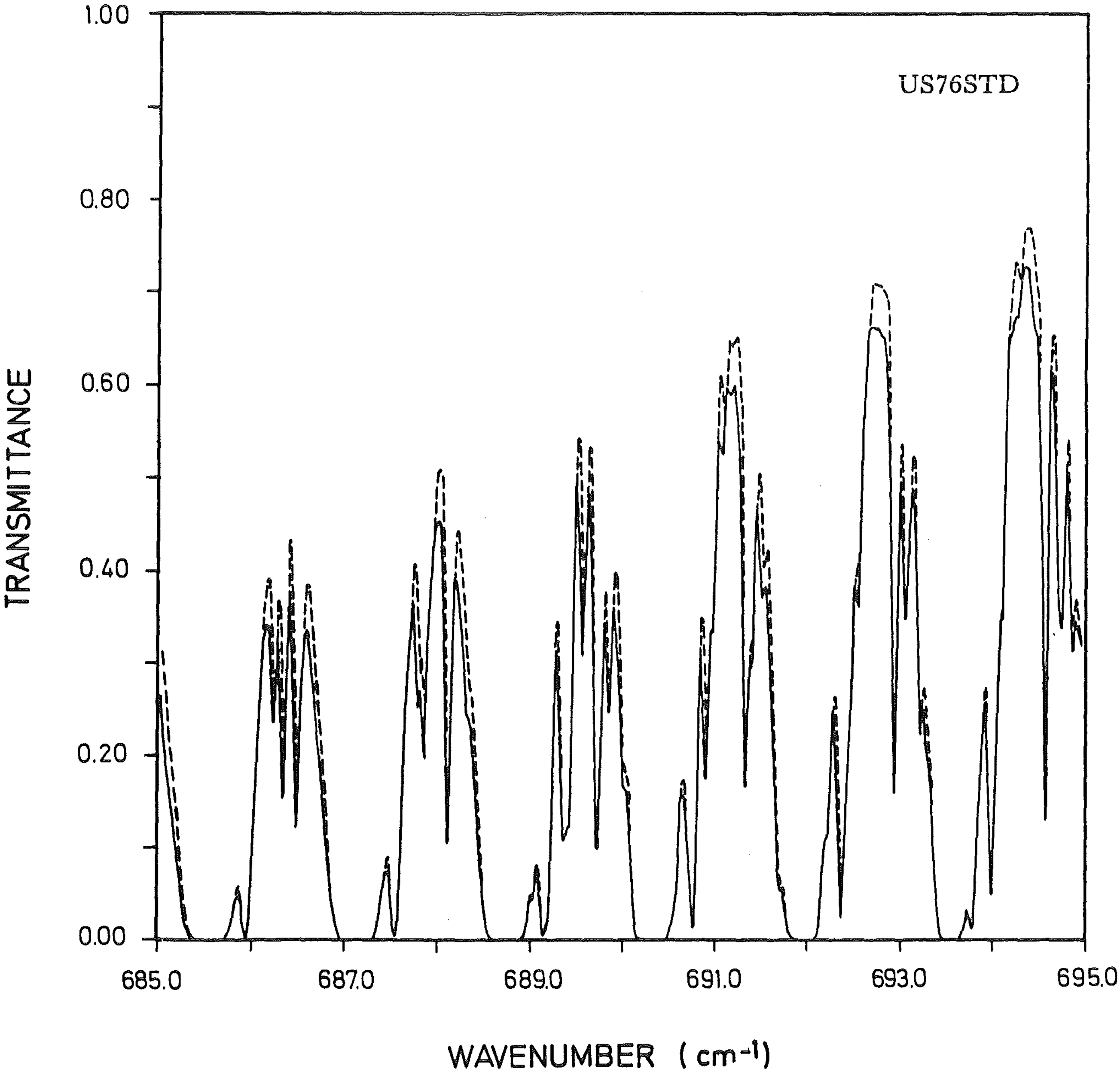

Fig. 4: Results of the calculations for CO_2 in the 685 to 695 cm^{-1} region; tangent height 30 km. Both plots are created with the DU - Program, using the Lorentzian line shape function and considering all the wings of lines within a range of ±25 cm^{-1} from the boundaries of the interval. The calculations were done with different temperature dependences of the line halfwidth.

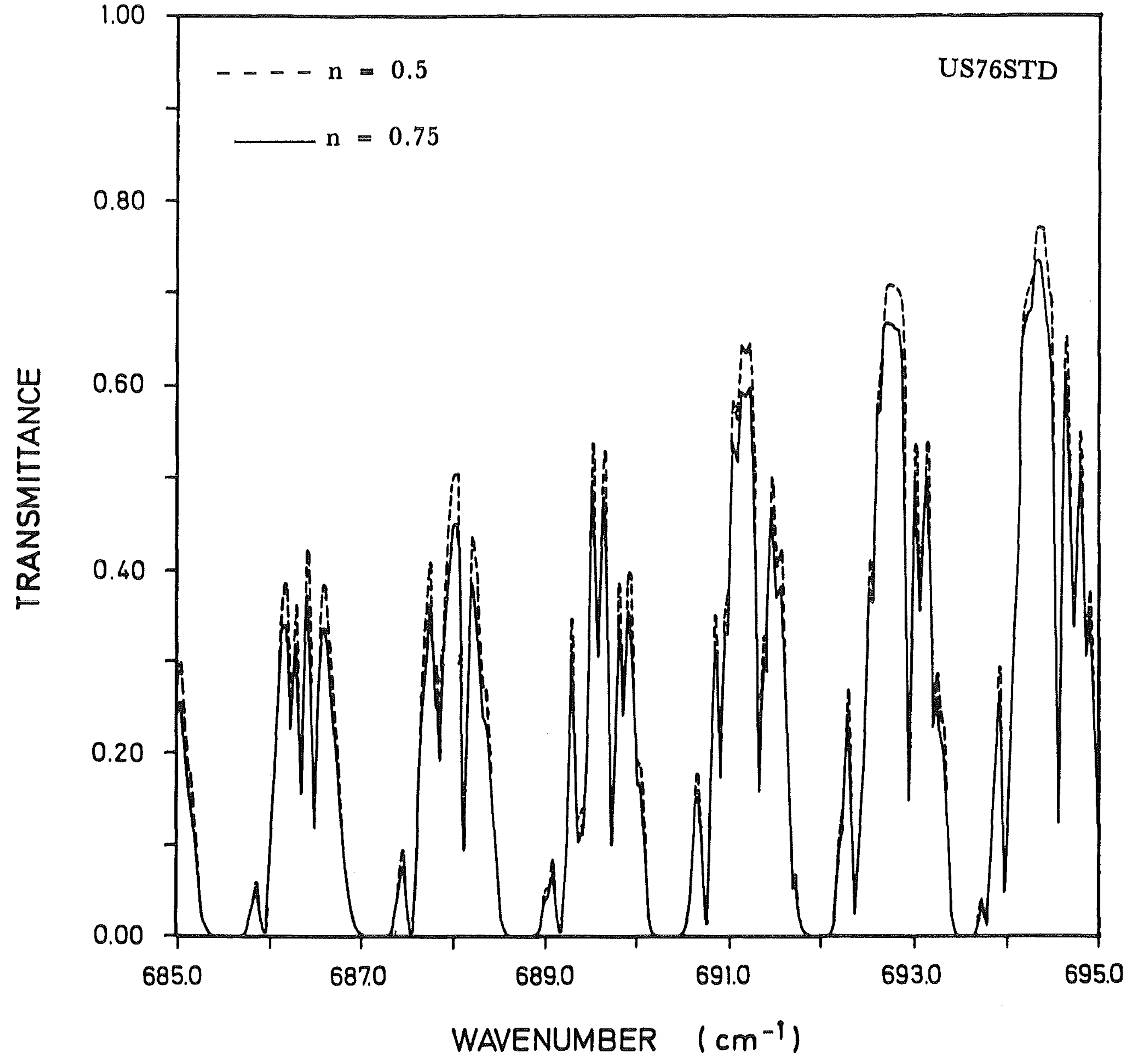

4.4 LINE WINGS AND CONTINUUM

Often the wings of lines outside the given spectral interval have a certain influence on the absorption within the interval. The ITRA participants use different methods of handling these line wings:

- The NCAR results in Exercise 1 do not include any contribution of lines from outside the given spectral interval. Thus, this program calculates the highest transmittance.
- The DU program takes into account the wings of lines in spectral intervals with a preselected width on both sides of the given spectral interval. This width is at least as large as the selected wings distance. This usually calculates less transmittance when compared with calculations with no contributions from lines outside the interval.
- The criterion of the MIM code is not the distance of a certain line to the given spectral interval, but the contribution of this line to the total absorption at any considered mesh point in the given spectral interval.
- AFGL's FASCOD2 line-by-line calculation directly convolves each line with an explicit line shape (described by four functions; see Code Description Section and Clough et al, 1986, 1987) within 25 cm^{-1} of line center. Because the sum of the four functions goes to zero at 25 cm^{-1}, the remaining non-zero offset within 25 cm^{-1} is stored with all contributions from line wings beyond 25 cm^{-1} in precalculated continua. The line shape χ- (or form) factor, a ratio which accounts for physical distortion from the exact Voigt profile, is embedded in the continua calculations.

The different handling of line wings from lines far off leads only to small differences in the gaps between the lines considering the CO_2 channels (see Fig. 1). In the case of the H_2O channel and a low tangent height the effect of the wings of lines outside the given spectral interval is remarkable as can be seen in Fig. 5. Large discrepancies in transmission appear for example around 1605 cm^{-1} which are mainly caused by the different handling of line wings but in addition the consideration of the H_2O continuum plays a certain role (AFGL calculations). Such effects can be expected for spectral intervals which are adjacent to strong bands. Also the conditions imposed by a low tangent height (relatively high pressure and broad Voigt lines) have to be met. At 30 km the continuum contributions are much less important, leading to excellent agreement as in Fig. 6.

The agreement between the results of the various computer codes has been further improved by agreeing on the same cutoff criterion. The second exercise was done with a cutoff criterion similar to the one in the DU Code (see Fig. 7).

No calculations for tangent heights of 10 km have been performed in ITRA2 (for explanation see page 9).

Fig. 5: Results of the intercomparison within the water vapour channel, z_{Min} = 10 km. As can be seen, the treatment of the wings of distant lines and associated χ – factor definitions are very important (ITRA 1).

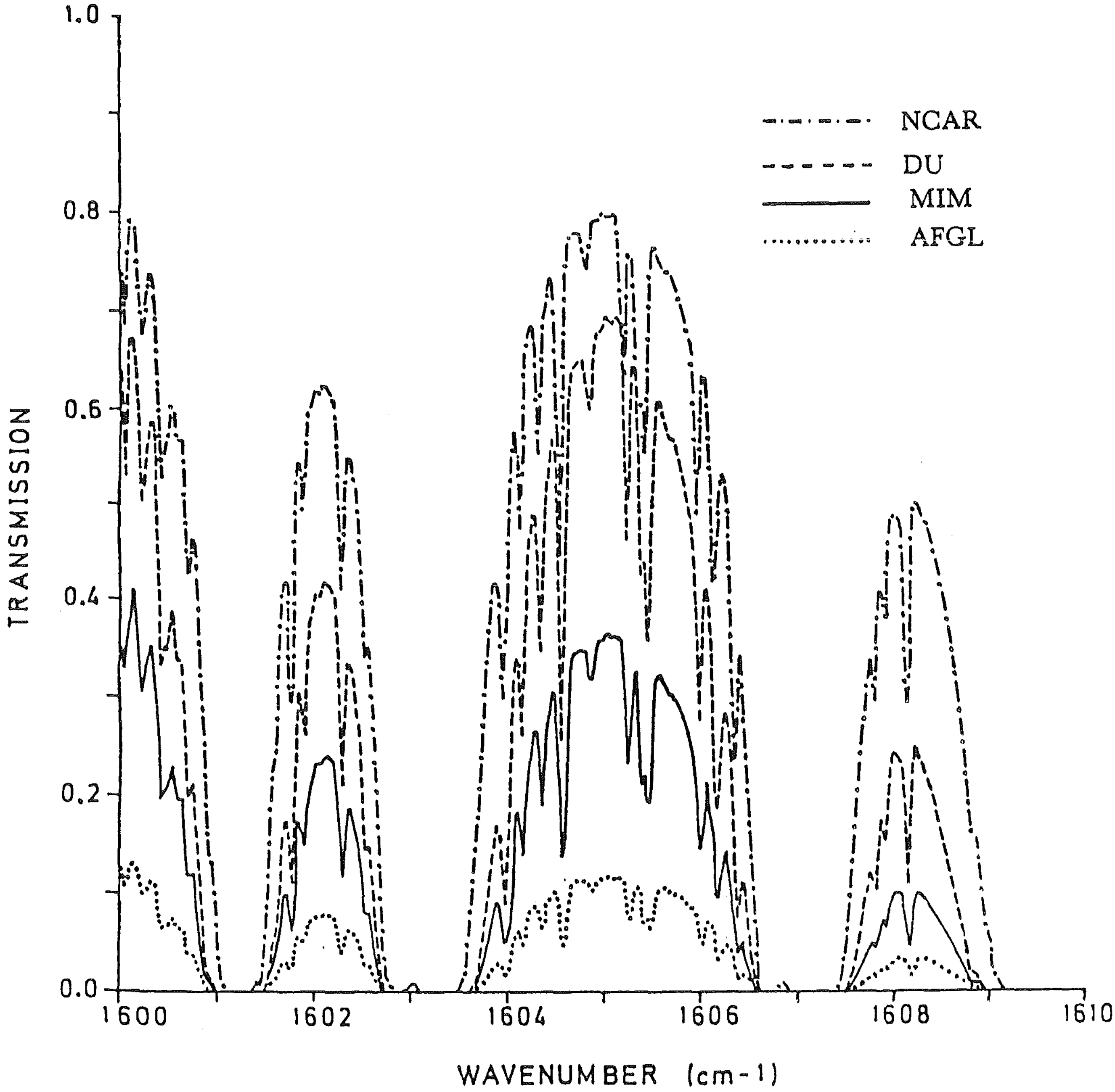

Fig. 6: Results of the intercomparison within the water vapour channel, z_{Min} = 30 km, radiance, ITRA1.

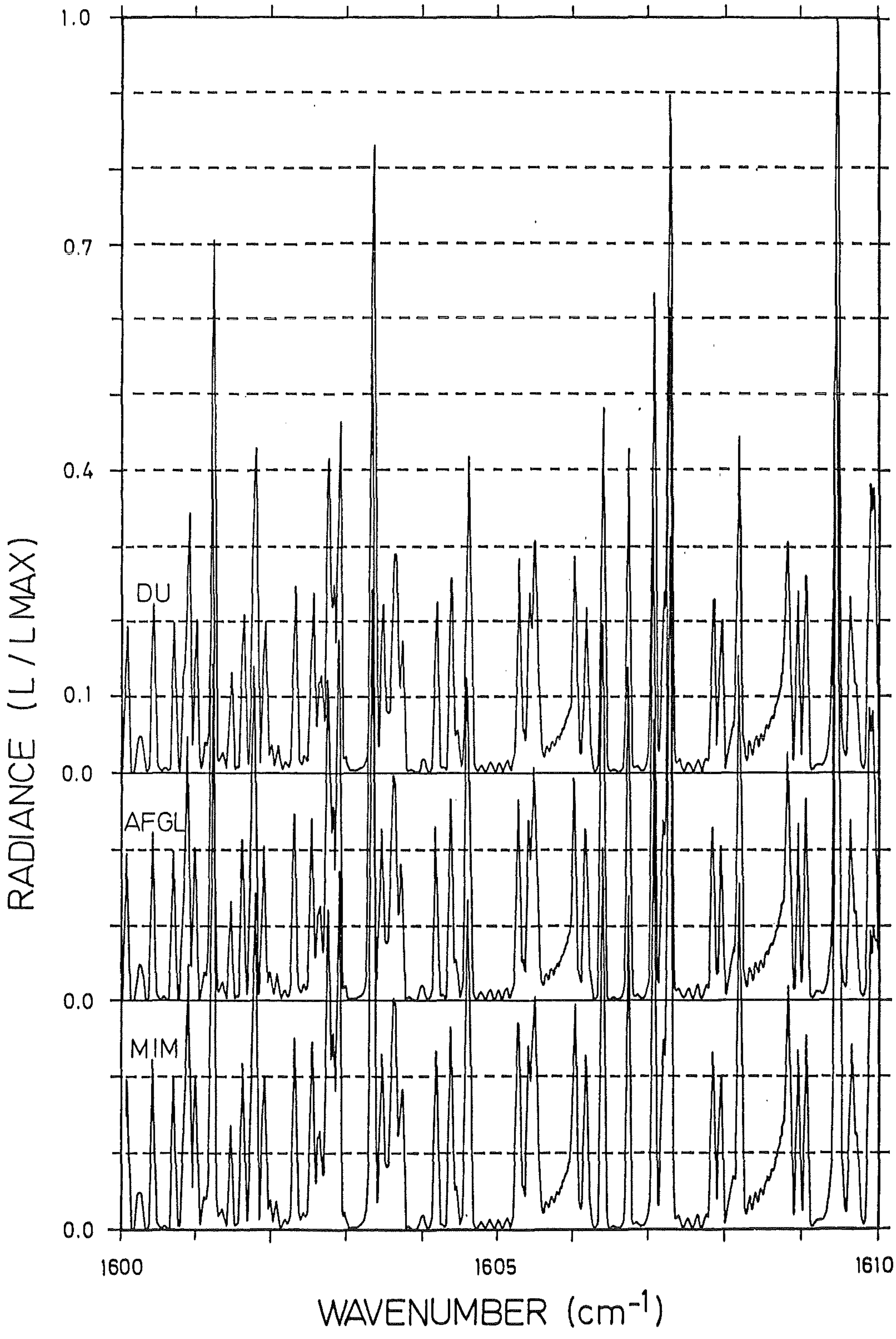

Fig. 7: Results of the intercomparison within the 685 – 695 cm^{-1} region, z_{Min} = 30 km, ITRA 2.

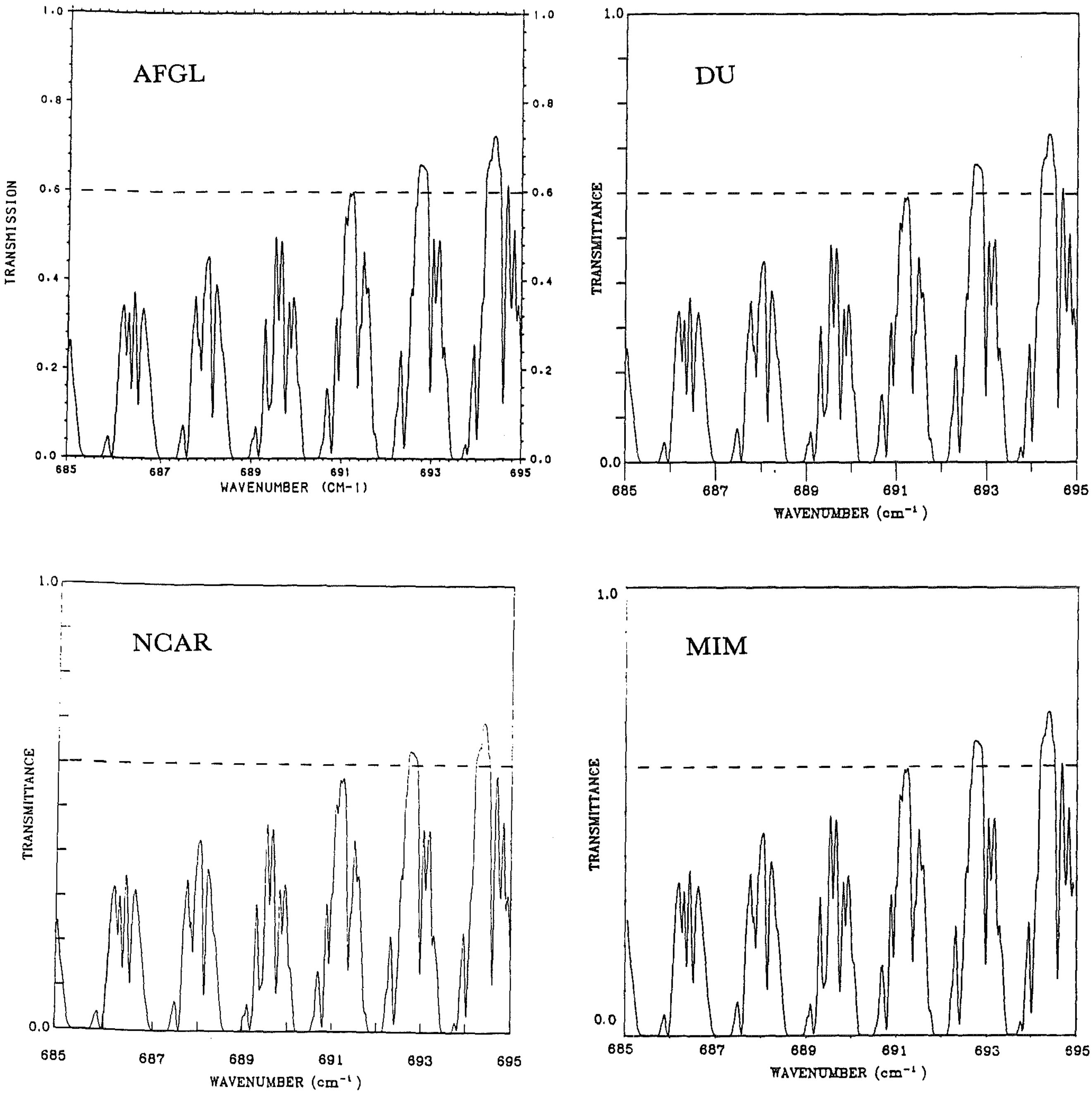

4.5 INTEGRAL VALUES

In the following, the integral values of transmittance and radiance are compared. Table 3 summarizes the results of transmittance calculations for the US Standard Atmosphere. It can be seen that the calculations are incomplete and that a more comprehensive comparison was only possible between AFGL and MIM results. In the first exercise the deviations in absorptance are mostly in the order of several percent but sometimes also in the range between 5 and 10 percent. The participants of the limb subgroup discussed these results and concluded that the deviations should be reduced to values below the 2% limit. Therefore, a second exercise was defined with specified spectral conditions. As expected, the ITRA2 integral transmittances in both the CO_2 and the H_2O channel fit much better than the ITRA1 results. The deviations in the CO_2 interval are now less than two percent; the results in the H_2O channel do not yet meet the 2% requirement.

The discrepancies between the integral radiances can be considered as subsequent effects of the results of transmittance calculations. The relative deviations of the integral absorptance are approximately as big as the relative deviations of the integral radiances in most cases . Small changes are probably caused by different numerical errors in the different computer codes (e.g. integration over wavelength, calculation of the Planck function).

The comparison of the calculations of exercise 1 yields the following results (see Table 4): The agreement between the NCAR and the MIM values is considerably better than between the AFGL and the NCAR/MIM values. With respect to the H_2O interval an input error seems to be the reason for the very small NCAR radiance values at tangent heights 50 km and 10 km.

As expected, the ITRA2 radiance values fit much better to each other.

Tab. 3: Integral transmittance values, US76Std – Atmosphere

interval	z_{Min}	transmittance	τ			deviation $\Delta(1-\tau)/(1-\bar{\tau})$
[cm⁻¹]	[km]	AFGL	DU	NCAR	MIM	MIM – AFGL
ITRA1						
685 – 695	50	0.895			0.890	– 0.046
	30	0.237			0.210	– 0.034
	10	0.000			0.000	0.000
715 – 725	50	0.917			0.912	– 0.058
	30	0.569			0.552	– 0.039
	10	0.0017			0.0005	– 0.001
732 – 764	50	0.984			0.984	0.000
	30	0.906			0.900	– 0.062
	10	0.193			0.185	– 0.010
1600 – 1610	50	0.9953	0.9943	0.9941	0.9949	– 0.082
	30	0.914	0.914	0.903	0.908	– 0.067
	10	0.043	0.203	0.107	0.134	0.093
ITRA2						
685 – 695	50	0.891			0.889	– 0.018
	30	0.192			0.190	– 0.002
1600 – 1610	50	0.9952			0.9950	– 0.048
	30	0.914			0.911	– 0.033

DU and NCAR did not use the triangular filter function

Tab. 4
Integral radiance [Watt/(cm^2·sr)]

spectral interval [cm^{-1}]	z_{min} [km]	AFGL	NCAR	MIM	DU	deviation [%] MIM – AFGL	MIM – NCAR	NCAR – AFGL
ITRA1								
685 – 695	50	$4.64 \cdot 10^{-6}$	$5.02 \cdot 10^{-6}$	$4.84 \cdot 10^{-6}$		+4.30	–3.59	+8.19
	30	$2.29 \cdot 10^{-5}$	$2.42 \cdot 10^{-5}$	$2.37 \cdot 10^{-5}$		+3.49	–2.89	+5.86
	10	$2.64 \cdot 10^{-5}$	$2.62 \cdot 10^{-5}$	$2.62 \cdot 10^{-5}$		+1.14	0.00	–0.76
715 – 725	50	$3.44 \cdot 10^{-6}$	$3.64 \cdot 10^{-6}$	$3.61 \cdot 10^{-6}$		+4.94	–0.82	+5.81
	30	$1.26 \cdot 10^{-5}$	$1.33 \cdot 10^{-5}$	$1.32 \cdot 10^{-5}$		+4.76	–0.75	+5.56
	10	$2.27 \cdot 10^{-5}$	$2.25 \cdot 10^{-5}$	$2.25 \cdot 10^{-5}$		–0.88	0.00	–2.88
732 – 764	50	$2.06 \cdot 10^{-6}$		$2.06 \cdot 10^{-6}$		±0.00		
	30	$8.04 \cdot 10^{-6}$		$8.59 \cdot 10^{-6}$		+6.84		
	10	$4.86 \cdot 10^{-5}$		$4.91 \cdot 10^{-6}$		+1.02		
1600 – 1610	50	$1.82 \cdot 10^{-8}$	$1.39 \cdot 10^{-9}$	$1.92 \cdot 10^{-8}$		+5.49	*)	+ *)
	30	$1.14 \cdot 10^{-7}$	$1.15 \cdot 10^{-7}$	$1.21 \cdot 10^{-7}$		+6.14	+5.22	+0.88
	10	$6.62 \cdot 10^{-7}$	$2.10 \cdot 10^{-7}$	$6.06 \cdot 10^{-7}$		–8.46	*)	*)
ITRA2								
685 – 695	50	$4.81 \cdot 10^{-6}$	$5.08 \cdot 10^{-6}$	$4.90 \cdot 10^{-6}$	$2.38 \cdot 10^{-5}$	+1.84	–3.67	+5.31
	30	$2.42 \cdot 10^{-5}$	$2.47 \cdot 10^{-5}$	$2.42 \cdot 10^{-5}$		±0.00	–2.07	+2.02
715 – 725	50		$3.69 \cdot 10^{-6}$	$3.63 \cdot 10^{-6}$			–1.65	
	30		$1.35 \cdot 10^{-5}$	$1.33 \cdot 10^{-5}$			–1.50	
732 – 764	50		$2.35 \cdot 10^{-6}$	$2.16 \cdot 10^{-6}$			–8.80	
	30		$8.92 \cdot 10^{-6}$	$8.62 \cdot 10^{-6}$			–3.48	
1600 – 1610	50	$1.82 \cdot 10^{-8}$		$1.86 \cdot 10^{-8}$		+2.19		
	30	$1.137 \cdot 10^{-7}$		$1.18 \cdot 10^{-7}$	$1.25 \cdot 10^{-7}$	+3.78		

*) probably input error

In order to get a comprehensive overview about all the calculations done during exercise 1 and 2 quicklook tables have been listed in Appendix B. These tables have been generated by comparing the different spectra and classifying the discrepancies between them. In general it is obvious that the agreement between the results of the different computer codes has been considerably improved by the specification of common spectroscopic parameters for exercise 2.

5. CONCLUSIONS AND RECOMMENDATIONS

The aim of the limb subgroup as defined during the workshop at the University of Maryland was to reduce the remaining discrepancies to less than 2% for each spectral radiance value as well as for the integral radiance value for the given spectral intervals. This aim has not been reached by carrying out two exercises. It can be concluded that considerable progress has been made to get consistently good agreement between the different computer codes but not all causes for discrepancies have been resolved.

Small differences between different computer codes are probably caused by the use of different numerical procedures (exercise 2). Larger discrepancies (up to five and more percent) may arise by the different handling of spectroscopic parameters (line shape, line wing effects, temperature dependence of half width etc). The first aim is to reach agreement between the results of different computer codes; this, however, would not imply that the radiation transfer can be simulated under realistic conditions in the atmosphere.

It is recommended that

1. the efforts in resolving the causes of discrepancies between different computer codes are continued in order to reduce them to values lower than the errors in transmittance/radiance measurements

2. the comparisons made up to now be extended to mass path calculations (e.g. CO, HNO_3), to high resolution calculations in the order of 0.01 cm^{-1}, to calculations for realistic atmospheric conditions (e.g. consideration of all absorbers in a given spectral interval) and to calculations within other spectral intervals (e.g. 10.5 – 12.5μm).

3. the investigation of far line wings is highly encouraged, in particular for laboratory measurements, and

4. very precise transmittance measurements with high spectral resolution (better than or equal to 0.1cm^{-1}) be performed in order to be able to check the results of the computer codes.

Furthermore it has been discussed at the workshop that the computer codes should be compared not only with respect to accuracy, but also with respect to speed and efficiency.

Appendix A: Tables of Input Values

1. Standard Atmosphere
   35 levels between 8 and 100 km

J	z(km)	p(mb)	T(K)	CO_2	H_2O	NO_2(day)
1	8.00	.35651E+03	236.22	.330E-03	.350E-03	.220E-10
2	10.00	.26499E+03	223.25	.330E-03	.600E-04	.230E-10
3	11.00	.22699E+03	216.77	.330E-03	.300E-04	.250E-10
4	12.00	.19399E+03	216.65	.330E-03	.130E-04	.290E-10
5	14.00	.14170E+03	216.65	.330E-03	.300E-05	.600E-10
6	16.00	.10352E+03	216.65	.330E-03	.315E-05	.350E-09
7	18.00	.75652E+02	216.65	.330E-03	.330E-05	.800E-09
8	20.00	.55293E+02	216.65	.330E-03	.345E-05	.140E-08
9	22.00	.40475E+02	218.57	.330E-03	.360E-05	.220E-08
10	24.00	.29717E+02	220.56	.330E-03	.375E-05	.300E-08
11	26.00	.21883E+02	222.54	.330E-03	.390E-05	.400E-08
12	28.00	.16161E+02	224.53	.330E-03	.405E-05	.530E-08
13	30.00	.11970E+02	226.51	.330E-03	.420E-05	.650E-08
14	32.00	.88906E+01	228.49	.330E-03	.440E-05	.750E-08
15	34.00	.66341E+01	233.74	.330E-03	.460E-05	.790E-08
16	36.00	.49852E+01	239.28	.330E-03	.480E-05	.790E-08
17	38.00	.37713E+01	244.82	.330E-03	.500E-05	.710E-08
18	40.00	.28714E+01	250.35	.330E-03	.515E-05	.550E-08
19	42.00	.21996E+01	255.88	.330E-03	.530E-05	.360E-08
20	44.00	.16949E+01	261.40	.330E-03	.545E-05	.180E-08
21	46.00	.13134E+01	266.93	.330E-03	.555E-05	.800E-09
22	48.00	.10229E+01	270.65	.330E-03	.565E-05	.360E-09
23	50.00	.79779E+00	270.65	.330E-03	.580E-05	.190E-09
24	52.50	.58438E+00	267.65	.330E-03	.590E-05	.900E-10
25	55.00	.42525E+00	260.77	.330E-03	.600E-05	.400E-10
26	57.50	.30691E+00	253.89	.330E-03	.610E-05	.180E-10
27	60.00	.21958E+00	247.02	.330E-03	.600E-05	.850E-11
28	62.50	.15567E+00	240.15	.330E-03	.580E-05	.380E-11
29	65.00	.10929E+00	233.29	.330E-03	.540E-05	.170E-11
30	67.50	.75953E-01	226.44	.330E-03	.500E-05	.800E-12
31	70.00	.52209E-01	219.59	.330E-03	.440E-05	.400E-12
32	75.00	.23881E-01	208.40	.330E-03	.320E-05	.190E-12
33	80.00	.10524E-01	198.64	.330E-03	.200E-05	.120E-12
34	90.00	.18359E-02	186.87	.330E-03	.600E-06	.100E-12
35	100.00	.32011E-03	195.08	.330E-03	.100E-06	.100E-12

1.1 Slant path for the Standard Atmosphere
Tangent height 10 km

CO_2

J	Z (KM)	PM (MB)	TM (K)	U (MOLEC/CM2)	SUM(U) (MOLEC/CM2)
1	100.00 - 90.00	.10838E-02	190.10	.6825E+17	.6825E+17
2	90.00 - 80.00	.62184E-02	194.02	.4151E+18	.4834E+18
3	80.00 - 75.00	.17236E-01	204.07	.6677E+18	.1151E+19
4	75.00 - 70.00	.38122E-01	214.60	.1469E+19	.2620E+19
5	70.00 - 67.50	.64116E-01	223.20	.1266E+19	.3886E+19
6	67.50 - 65.00	.92672E-01	230.05	.1816E+19	.5702E+19
7	65.00 - 62.50	.13255E+00	236.90	.2582E+19	.8284E+19
8	62.50 - 60.00	.18773E+00	243.76	.3641E+19	.1192E+20
9	60.00 - 57.50	.26340E+00	250.63	.5097E+19	.1702E+20
10	57.50 - 55.00	.36630E+00	257.50	.7086E+19	.2411E+20
11	55.00 - 52.50	.50513E+00	264.38	.9790E+19	.3390E+20
12	52.50 - 50.00	.69154E+00	269.22	.1351E+20	.4741E+20
13	50.00 - 48.00	.91075E+00	270.65	.1465E+20	.6206E+20
14	48.00 - 46.00	.11687E+01	268.72	.1940E+20	.8146E+20
15	46.00 - 44.00	.15049E+01	264.05	.2619E+20	.1077E+21
16	44.00 - 42.00	.19483E+01	258.53	.3567E+20	.1433E+21
17	42.00 - 40.00	.25370E+01	253.00	.4897E+20	.1923E+21
18	40.00 - 38.00	.33236E+01	247.47	.6782E+20	.2601E+21
19	38.00 - 36.00	.43815E+01	241.93	.9480E+20	.3549E+21
20	36.00 - 34.00	.58144E+01	236.39	.1338E+21	.4887E+21
21	34.00 - 32.00	.77694E+01	230.99	.1910E+21	.6797E+21
22	32.00 - 30.00	.10441E+02	227.45	.2728E+21	.9526E+21
23	30.00 - 28.00	.14081E+02	225.47	.3906E+21	.1343E+22
24	28.00 - 26.00	.19046E+02	223.49	.5643E+21	.1907E+22
25	26.00 - 24.00	.25838E+02	221.50	.8234E+21	.2731E+22
26	24.00 - 22.00	.35157E+02	219.51	.1216E+22	.3947E+22
27	22.00 - 20.00	.47983E+02	217.56	.1825E+22	.5773E+22
28	20.00 - 18.00	.65639E+02	216.65	.2780E+22	.8553E+22
29	18.00 - 16.00	.89881E+02	216.65	.4334E+22	.1289E+23
30	16.00 - 14.00	.12318E+03	216.65	.7073E+22	.1996E+23
31	14.00 - 12.00	.16918E+03	216.65	.1270E+23	.3266E+23
32	12.00 - 11.00	.21132E+03	216.72	.1130E+23	.4396E+23
33	11.00 - 10.00	.25214E+03	221.12	.3187E+23	.7583E+23
34	10.00 - 11.00	.25214E+03	221.12	.3187E+23	.1077E+24
35	11.00 - 12.00	.21132E+03	216.72	.1130E+23	.1190E+24
36	12.00 - 14.00	.16918E+03	216.65	.1270E+23	.1317E+24
37	14.00 - 16.00	.12318E+03	216.65	.7073E+22	.1388E+24
38	16.00 - 18.00	.89881E+02	216.65	.4334E+22	.1431E+24
39	18.00 - 20.00	.65639E+02	216.65	.2780E+22	.1459E+24
40	20.00 - 22.00	.47983E+02	217.56	.1825E+22	.1477E+24
41	22.00 - 24.00	.35157E+02	219.51	.1216E+22	.1489E+24
42	24.00 - 26.00	.25838E+02	221.50	.8234E+21	.1498E+24
43	26.00 - 28.00	.19046E+02	223.49	.5643E+21	.1503E+24
44	28.00 - 30.00	.14081E+02	225.47	.3906E+21	.1507E+24
45	30.00 - 32.00	.10441E+02	227.45	.2728E+21	.1510E+24
46	32.00 - 34.00	.77694E+01	230.99	.1910E+21	.1512E+24
47	34.00 - 36.00	.58144E+01	236.39	.1338E+21	.1513E+24
48	36.00 - 38.00	.43815E+01	241.93	.9480E+20	.1514E+24
49	38.00 - 40.00	.33236E+01	247.47	.6782E+20	.1515E+24
50	40.00 - 42.00	.25370E+01	253.00	.4897E+20	.1515E+24
51	42.00 - 44.00	.19483E+01	258.53	.3567E+20	.1516E+24
52	44.00 - 46.00	.15049E+01	264.05	.2619E+20	.1516E+24
53	46.00 - 48.00	.11687E+01	268.72	.1940E+20	.1516E+24
54	48.00 - 50.00	.91075E+00	270.65	.1465E+20	.1516E+24
55	50.00 - 52.50	.69154E+00	269.22	.1351E+20	.1516E+24
56	52.50 - 55.00	.50513E+00	264.38	.9790E+19	.1516E+24
57	55.00 - 57.50	.36630E+00	257.50	.7086E+19	.1517E+24
58	57.50 - 60.00	.26340E+00	250.63	.5097E+19	.1517E+24
59	60.00 - 62.50	.18773E+00	243.76	.3641E+19	.1517E+24
60	62.50 - 65.00	.13255E+00	236.90	.2582E+19	.1517E+24
61	65.00 - 67.50	.92672E-01	230.05	.1816E+19	.1517E+24
62	67.50 - 70.00	.64116E-01	223.20	.1266E+19	.1517E+24
63	70.00 - 75.00	.38122E-01	214.60	.1469E+19	.1517E+24
64	75.00 - 80.00	.17236E-01	204.07	.6677E+18	.1517E+24
65	80.00 - 90.00	.62184E-02	194.02	.4151E+18	.1517E+24
66	90.00 - 100.00	.10838E-02	190.10	.6825E+17	.1517E+24

H_2O

J	Z (KM)	PM (MB)	TM (K)	U (MOLEC/CM2)	SUM(U) (MOLEC/CM2)
1	100.00 - 90.00	.12142E-02	189.40	.8342E+14	.8342E+14
2	90.00 - 80.00	.68008E-02	194.80	.1824E+16	.1908E+16
3	80.00 - 75.00	.17662E-01	204.38	.5398E+16	.7306E+16
4	75.00 - 70.00	.38746E-01	214.85	.1721E+17	.2451E+17
5	70.00 - 67.50	.64331E-01	223.26	.1810E+17	.4261E+17
6	67.50 - 65.00	.92855E-01	230.08	.2867E+17	.7128E+17
7	65.00 - 62.50	.13279E+00	236.94	.4390E+17	.1152E+18
8	62.50 - 60.00	.18789E+00	243.78	.6515E+17	.1803E+18
9	60.00 - 57.50	.26350E+00	250.64	.9349E+17	.2738E+18
10	57.50 - 55.00	.36616E+00	257.49	.1299E+18	.4037E+18
11	55.00 - 52.50	.50494E+00	264.37	.1765E+18	.5801E+18
12	52.50 - 50.00	.69128E+00	269.22	.2395E+18	.8196E+18
13	50.00 - 48.00	.91033E+00	270.65	.2540E+18	.1074E+19
14	48.00 - 46.00	.11683E+01	268.72	.3291E+18	.1403E+19
15	46.00 - 44.00	.15044E+01	264.06	.4363E+18	.1839E+19
16	44.00 - 42.00	.19473E+01	258.54	.5806E+18	.2420E+19
17	42.00 - 40.00	.25357E+01	253.01	.7749E+18	.3195E+19
18	40.00 - 38.00	.33217E+01	247.48	.1042E+19	.4237E+19
19	38.00 - 36.00	.43779E+01	241.94	.1406E+19	.5643E+19
20	36.00 - 34.00	.58094E+01	236.40	.1904E+19	.7547E+19
21	34.00 - 32.00	.77622E+01	231.01	.2602E+19	.1015E+20
22	32.00 - 30.00	.10431E+02	227.46	.3551E+19	.1370E+20
23	30.00 - 28.00	.14071E+02	225.47	.4878E+19	.1858E+20
24	28.00 - 26.00	.19031E+02	223.49	.6790E+19	.2537E+20
25	26.00 - 24.00	.25816E+02	221.51	.9534E+19	.3490E+20
26	24.00 - 22.00	.35125E+02	219.52	.1353E+20	.4844E+20
27	22.00 - 20.00	.47938E+02	217.56	.1947E+20	.6791E+20
28	20.00 - 18.00	.65574E+02	216.65	.2840E+20	.9631E+20
29	18.00 - 16.00	.89787E+02	216.65	.4229E+20	.1386E+21
30	16.00 - 14.00	.12305E+03	216.65	.6579E+20	.2044E+21
31	14.00 - 12.00	.17370E+03	216.65	.3262E+21	.5306E+21
32	12.00 - 11.00	.21318E+03	216.72	.7573E+21	.1288E+22
33	11.00 - 10.00	.25403E+03	221.44	.4840E+22	.6128E+22
34	10.00 - 11.00	.25403E+03	221.44	.4840E+22	.1097E+23
35	11.00 - 12.00	.21318E+03	216.72	.7573E+21	.1173E+23
36	12.00 - 14.00	.17370E+03	216.65	.3262E+21	.1205E+23
37	14.00 - 16.00	.12305E+03	216.65	.6579E+20	.1212E+23
38	16.00 - 18.00	.89787E+02	216.65	.4229E+20	.1216E+23
39	18.00 - 20.00	.65574E+02	216.65	.2840E+20	.1219E+23
40	20.00 - 22.00	.47938E+02	217.56	.1947E+20	.1221E+23
41	22.00 - 24.00	.35125E+02	219.52	.1353E+20	.1222E+23
42	24.00 - 26.00	.25816E+02	221.51	.9534E+19	.1223E+23
43	26.00 - 28.00	.19031E+02	223.49	.6790E+19	.1224E+23
44	28.00 - 30.00	.14071E+02	225.47	.4878E+19	.1224E+23
45	30.00 - 32.00	.10431E+02	227.46	.3551E+19	.1225E+23
46	32.00 - 34.00	.77622E+01	231.01	.2602E+19	.1225E+23
47	34.00 - 36.00	.58094E+01	236.40	.1904E+19	.1225E+23
48	36.00 - 38.00	.43779E+01	241.94	.1406E+19	.1225E+23
49	38.00 - 40.00	.33217E+01	247.48	.1042E+19	.1225E+23
50	40.00 - 42.00	.25357E+01	253.01	.7749E+18	.1225E+23
51	42.00 - 44.00	.19473E+01	258.54	.5806E+18	.1225E+23
52	44.00 - 46.00	.15044E+01	264.06	.4363E+18	.1226E+23
53	46.00 - 48.00	.11683E+01	268.72	.3291E+18	.1226E+23
54	48.00 - 50.00	.91033E+00	270.65	.2540E+18	.1226E+23
55	50.00 - 52.50	.69128E+00	269.22	.2395E+18	.1226E+23
56	52.50 - 55.00	.50494E+00	264.37	.1765E+18	.1226E+23
57	55.00 - 57.50	.36616E+00	257.49	.1299E+18	.1226E+23
58	57.50 - 60.00	.26350E+00	250.64	.9349E+17	.1226E+23
59	60.00 - 62.50	.18789E+00	243.78	.6515E+17	.1226E+23
60	62.50 - 65.00	.13279E+00	236.94	.4390E+17	.1226E+23
61	65.00 - 67.50	.92855E-01	230.08	.2867E+17	.1226E+23
62	67.50 - 70.00	.64331E-01	223.26	.1810E+17	.1226E+23
63	70.00 - 75.00	.38746E-01	214.85	.1721E+17	.1226E+23
64	75.00 - 80.00	.17662E-01	204.38	.5398E+16	.1226E+23
65	80.00 - 90.00	.68008E-02	194.80	.1824E+16	.1226E+23
66	90.00 -100.00	.12142E-02	189.40	.8342E+14	.1226E+23

NO_2 Day

J	Z (KM)	PM (MB)	TM (K)	U (MOLEC/CM2)	SUM(U) (MOLEC/CM2)
1	100.00 - 90.00	.10838E-02	190.10	.2068E+08	.2068E+08
2	90.00 - 80.00	.63260E-02	194.16	.1411E+09	.1618E+09
3	80.00 - 75.00	.17653E-01	204.38	.3216E+09	.4834E+09
4	75.00 - 70.00	.39498E-01	215.15	.1364E+10	.1848E+10
5	70.00 - 67.50	.65223E-01	223.52	.2345E+10	.4192E+10
6	67.50 - 65.00	.94351E-01	230.39	.7010E+10	.1120E+11
7	65.00 - 62.50	.13503E+00	237.27	.2195E+11	.3315E+11
8	62.50 - 60.00	.19115E+00	244.13	.6918E+11	.1023E+12
9	60.00 - 57.50	.26779E+00	250.97	.2083E+12	.3107E+12
10	57.50 - 55.00	.37259E+00	257.87	.6343E+12	.9450E+12
11	55.00 - 52.50	.51371E+00	264.75	.1964E+13	.2909E+13
12	52.50 - 50.00	.70223E+00	269.37	.5831E+13	.8740E+13
13	50.00 - 48.00	.92057E+00	270.65	.1235E+14	.2109E+14
14	48.00 - 46.00	.11842E+01	268.52	.3460E+14	.5569E+14
15	46.00 - 44.00	.15256E+01	263.76	.1047E+15	.1604E+15
16	44.00 - 42.00	.19720E+01	258.27	.2958E+15	.4562E+15
17	42.00 - 40.00	.25569E+01	252.84	.6811E+15	.1137E+16
18	40.00 - 38.00	.33398E+01	247.37	.1302E+16	.2439E+16
19	38.00 - 36.00	.43907E+01	241.89	.2160E+16	.4599E+16
20	36.00 - 34.00	.58144E+01	236.39	.3204E+16	.7803E+16
21	34.00 - 32.00	.77610E+01	231.01	.4451E+16	.1225E+17
22	32.00 - 30.00	.10409E+02	227.47	.5768E+16	.1802E+17
23	30.00 - 28.00	.14020E+02	225.50	.6949E+16	.2497E+17
24	28.00 - 26.00	.18931E+02	223.53	.7895E+16	.3286E+17
25	26.00 - 24.00	.25677E+02	221.54	.8668E+16	.4153E+17
26	24.00 - 22.00	.34917E+02	219.56	.9504E+16	.5104E+17
27	22.00 - 20.00	.47504E+02	217.62	.9831E+16	.6087E+17
28	20.00 - 18.00	.64828E+02	216.65	.9116E+16	.6998E+17
29	18.00 - 16.00	.88268E+02	216.65	.7360E+16	.7734E+17
30	16.00 - 14.00	.11905E+03	216.65	.4165E+16	.8151E+17
31	14.00 - 12.00	.16642E+03	216.65	.1657E+16	.8317E+17
32	12.00 - 11.00	.21096E+03	216.72	.9196E+15	.8408E+17
33	11.00 - 10.00	.25187E+03	221.07	.2285E+16	.8637E+17
34	10.00 - 11.00	.25187E+03	221.07	.2285E+16	.8865E+17
35	11.00 - 12.00	.21096E+03	216.72	.9196E+15	.8957E+17
36	12.00 - 14.00	.16642E+03	216.65	.1657E+16	.9123E+17
37	14.00 - 16.00	.11905E+03	216.65	.4165E+16	.9540E+17
38	16.00 - 18.00	.88268E+02	216.65	.7360E+16	.1028E+18
39	18.00 - 20.00	.64828E+02	216.65	.9116E+16	.1119E+18
40	20.00 - 22.00	.47504E+02	217.62	.9831E+16	.1217E+18
41	22.00 - 24.00	.34917E+02	219.56	.9504E+16	.1312E+18
42	24.00 - 26.00	.25677E+02	221.54	.8668E+16	.1399E+18
43	26.00 - 28.00	.18931E+02	223.53	.7895E+16	.1478E+18
44	28.00 - 30.00	.14020E+02	225.50	.6949E+16	.1547E+18
45	30.00 - 32.00	.10409E+02	227.47	.5768E+16	.1605E+18
46	32.00 - 34.00	.77610E+01	231.01	.4451E+16	.1649E+18
47	34.00 - 36.00	.58144E+01	236.39	.3204E+16	.1681E+18
48	36.00 - 38.00	.43907E+01	241.89	.2160E+16	.1703E+18
49	38.00 - 40.00	.33398E+01	247.37	.1302E+16	.1716E+18
50	40.00 - 42.00	.25569E+01	252.84	.6811E+15	.1723E+18
51	42.00 - 44.00	.19720E+01	258.27	.2958E+15	.1726E+18
52	44.00 - 46.00	.15256E+01	263.76	.1047E+15	.1727E+18
53	46.00 - 48.00	.11842E+01	268.52	.3460E+14	.1727E+18
54	48.00 - 50.00	.92057E+00	270.65	.1235E+14	.1727E+18
55	50.00 - 52.50	.70223E+00	269.37	.5831E+13	.1727E+18
56	52.50 - 55.00	.51371E+00	264.75	.1964E+13	.1727E+18
57	55.00 - 57.50	.37259E+00	257.87	.6343E+12	.1727E+18
58	57.50 - 60.00	.26779E+00	250.97	.2083E+12	.1727E+18
59	60.00 - 62.50	.19115E+00	244.13	.6918E+11	.1727E+18
60	62.50 - 65.00	.13503E+00	237.27	.2195E+11	.1727E+18
61	65.00 - 67.50	.94351E-01	230.39	.7010E+10	.1727E+18
62	67.50 - 70.00	.65223E-01	223.52	.2345E+10	.1727E+18
63	70.00 - 75.00	.39498E-01	215.15	.1364E+10	.1727E+18
64	75.00 - 80.00	.17653E-01	204.38	.3216E+09	.1727E+18
65	80.00 - 90.00	.63260E-02	194.16	.1411E+09	.1727E+18
66	90.00 -100.00	.10838E-02	190.10	.2068E+08	.1727E+18

1.2 Slant path for the Standard Atmosphere
Tangent height 30 km

CO_2

J	Z (KM)	PM (MB)	TM (K)	U (MOLEC/CM2)	SUM(U) (MOLEC/CM2)
1	100.00 - 90.00	.10857E-02	190.09	.7791E+17	.7791E+17
2	90.00 - 80.00	.62332E-02	194.04	.4840E+18	.5619E+18
3	80.00 - 75.00	.17251E-01	204.08	.7928E+18	.1355E+19
4	75.00 - 70.00	.38160E-01	214.62	.1774E+19	.3129E+19
5	70.00 - 67.50	.64134E-01	223.20	.1551E+19	.4680E+19
6	67.50 - 65.00	.92701E-01	230.05	.2250E+19	.6930E+19
7	65.00 - 62.50	.13260E+00	236.91	.3241E+19	.1017E+20
8	62.50 - 60.00	.18780E+00	243.77	.4636E+19	.1481E+20
9	60.00 - 57.50	.26351E+00	250.64	.6599E+19	.2141E+20
10	57.50 - 55.00	.36647E+00	257.51	.9349E+19	.3076E+20
11	55.00 - 52.50	.50540E+00	264.39	.1321E+20	.4396E+20
12	52.50 - 50.00	.69197E+00	269.23	.1871E+20	.6267E+20
13	50.00 - 48.00	.91118E+00	270.65	.2084E+20	.8351E+20
14	48.00 - 46.00	.11694E+01	268.71	.2842E+20	.1119E+21
15	46.00 - 44.00	.15060E+01	264.04	.3972E+20	.1516E+21
16	44.00 - 42.00	.19500E+01	258.51	.5642E+20	.2081E+21
17	42.00 - 40.00	.25399E+01	252.98	.8163E+20	.2897E+21
18	40.00 - 38.00	.33285E+01	247.43	.1209E+21	.4106E+21
19	38.00 - 36.00	.43908E+01	241.88	.1851E+21	.5958E+21
20	36.00 - 34.00	.58338E+01	236.32	.2985E+21	.8943E+21
21	34.00 - 32.00	.78195E+01	230.88	.5339E+21	.1428E+22
22	32.00 - 30.00	.10942E+02	227.14	.1831E+22	.3259E+22
23	30.00 - 32.00	.10942E+02	227.14	.1831E+22	.5090E+22
24	32.00 - 34.00	.78195E+01	230.88	.5339E+21	.5624E+22
25	34.00 - 36.00	.58338E+01	236.32	.2985E+21	.5922E+22
26	36.00 - 38.00	.43908E+01	241.88	.1851E+21	.6107E+22
27	38.00 - 40.00	.33285E+01	247.43	.1209E+21	.6228E+22
28	40.00 - 42.00	.25399E+01	252.98	.8163E+20	.6310E+22
29	42.00 - 44.00	.19500E+01	258.51	.5642E+20	.6366E+22
30	44.00 - 46.00	.15060E+01	264.04	.3972E+20	.6406E+22
31	46.00 - 48.00	.11694E+01	268.71	.2842E+20	.6435E+22
32	48.00 - 50.00	.91118E+00	270.65	.2084E+20	.6455E+22
33	50.00 - 52.50	.69197E+00	269.23	.1871E+20	.6474E+22
34	52.50 - 55.00	.50540E+00	264.39	.1321E+20	.6487E+22
35	55.00 - 57.50	.36647E+00	257.51	.9349E+19	.6497E+22
36	57.50 - 60.00	.26351E+00	250.64	.6599E+19	.6503E+22
37	60.00 - 62.50	.18780E+00	243.77	.4636E+19	.6508E+22
38	62.50 - 65.00	.13260E+00	236.91	.3241E+19	.6511E+22
39	65.00 - 67.50	.92701E-01	230.05	.2250E+19	.6513E+22
40	67.50 - 70.00	.64134E-01	223.20	.1551E+19	.6515E+22
41	70.00 - 75.00	.38160E-01	214.62	.1774E+19	.6517E+22
42	75.00 - 80.00	.17251E-01	204.08	.7928E+18	.6517E+22
43	80.00 - 90.00	.62332E-02	194.04	.4840E+18	.6518E+22
44	90.00 - 100.00	.10857E-02	190.09	.7791E+17	.6518E+22

H_2O

J	Z (KM)	PM (MB)	TM (K)	U (MOLEC/CM2)	SUM(U) (MOLEC/CM2)
1	100.00 - 90.00	.12161E-02	189.39	.9537E+14	.9537E+14
2	90.00 - 80.00	.68154E-02	194.82	.2130E+16	.2226E+16
3	80.00 - 75.00	.17676E-01	204.39	.6413E+16	.8639E+16
4	75.00 - 70.00	.38784E-01	214.86	.2079E+17	.2943E+17
5	70.00 - 67.50	.64349E-01	223.27	.2218E+17	.5161E+17
6	67.50 - 65.00	.92884E-01	230.09	.3553E+17	.8713E+17
7	65.00 - 62.50	.13284E+00	236.94	.5510E+17	.1422E+18
8	62.50 - 60.00	.18796E+00	243.79	.8297E+17	.2252E+18
9	60.00 - 57.50	.26361E+00	250.65	.1210E+18	.3462E+18
10	57.50 - 55.00	.36634E+00	257.50	.1713E+18	.5176E+18
11	55.00 - 52.50	.50521E+00	264.38	.2380E+18	.7556E+18
12	52.50 - 50.00	.69171E+00	269.23	.3315E+18	.1087E+19
13	50.00 - 48.00	.91076E+00	270.65	.3614E+18	.1448E+19
14	48.00 - 46.00	.11690E+01	268.71	.4821E+18	.1931E+19
15	46.00 - 44.00	.15055E+01	264.05	.6616E+18	.2592E+19
16	44.00 - 42.00	.19490E+01	258.52	.9183E+18	.3511E+19
17	42.00 - 40.00	.25385E+01	252.99	.1292E+19	.4802E+19
18	40.00 - 38.00	.33266E+01	247.45	.1858E+19	.6660E+19
19	38.00 - 36.00	.43872E+01	241.90	.2746E+19	.9406E+19
20	36.00 - 34.00	.58288E+01	236.34	.4245E+19	.1365E+20
21	34.00 - 32.00	.78122E+01	230.89	.7265E+19	.2092E+20
22	32.00 - 30.00	.10930E+02	227.14	.2365E+20	.4457E+20
23	30.00 - 32.00	.10930E+02	227.14	.2365E+20	.6822E+20
24	32.00 - 34.00	.78122E+01	230.89	.7265E+19	.7549E+20
25	34.00 - 36.00	.58288E+01	236.34	.4245E+19	.7973E+20
26	36.00 - 38.00	.43872E+01	241.90	.2746E+19	.8248E+20
27	38.00 - 40.00	.33266E+01	247.45	.1858E+19	.8434E+20
28	40.00 - 42.00	.25385E+01	252.99	.1292E+19	.8563E+20
29	42.00 - 44.00	.19490E+01	258.52	.9183E+18	.8655E+20
30	44.00 - 46.00	.15055E+01	264.05	.6616E+18	.8721E+20
31	46.00 - 48.00	.11690E+01	268.71	.4821E+18	.8769E+20
32	48.00 - 50.00	.91076E+00	270.65	.3614E+18	.8805E+20
33	50.00 - 52.50	.69171E+00	269.23	.3315E+18	.8839E+20
34	52.50 - 55.00	.50521E+00	264.38	.2380E+18	.8862E+20
35	55.00 - 57.50	.36634E+00	257.50	.1713E+18	.8879E+20
36	57.50 - 60.00	.26361E+00	250.65	.1210E+18	.8892E+20
37	60.00 - 62.50	.18796E+00	243.79	.8297E+17	.8900E+20
38	62.50 - 65.00	.13284E+00	236.94	.5510E+17	.8905E+20
39	65.00 - 67.50	.92884E-01	230.09	.3553E+17	.8909E+20
40	67.50 - 70.00	.64349E-01	223.27	.2218E+17	.8911E+20
41	70.00 - 75.00	.38784E-01	214.86	.2079E+17	.8913E+20
42	75.00 - 80.00	.17676E-01	204.39	.6413E+16	.8914E+20
43	80.00 - 90.00	.68154E-02	194.82	.2130E+16	.8914E+20
44	90.00 -100.00	.12161E-02	189.39	.9537E+14	.8914E+20

NO_2 Day

J	Z (KM)	PM (MB)	TM (K)	U (MOLEC/CM2)	SUM(U) (MOLEC/CM2)
1	100.00 - 90.00	.10857E-02	190.09	.2361E+08	.2361E+08
2	90.00 - 80.00	.63409E-02	194.18	.1645E+09	.1881E+09
3	80.00 - 75.00	.17668E-01	204.39	.3821E+09	.5703E+09
4	75.00 - 70.00	.39537E-01	215.16	.1649E+10	.2220E+10
5	70.00 - 67.50	.65242E-01	223.52	.2874E+10	.5093E+10
6	67.50 - 65.00	.94380E-01	230.40	.8692E+10	.1378E+11
7	65.00 - 62.50	.13508E+00	237.27	.2757E+11	.4135E+11
8	62.50 - 60.00	.19122E+00	244.14	.8817E+11	.1295E+12
9	60.00 - 57.50	.26790E+00	250.98	.2699E+12	.3995E+12
10	57.50 - 55.00	.37277E+00	257.88	.8378E+12	.1237E+13
11	55.00 - 52.50	.51399E+00	264.76	.2653E+13	.3890E+13
12	52.50 - 50.00	.70268E+00	269.38	.8084E+13	.1197E+14
13	50.00 - 48.00	.92101E+00	270.65	.1760E+14	.2957E+14
14	48.00 - 46.00	.11849E+01	268.51	.5077E+14	.8034E+14
15	46.00 - 44.00	.15266E+01	263.74	.1592E+15	.2395E+15
16	44.00 - 42.00	.19738E+01	258.25	.4689E+15	.7084E+15
17	42.00 - 40.00	.25598E+01	252.81	.1137E+16	.1846E+16
18	40.00 - 38.00	.33449E+01	247.33	.2324E+16	.4170E+16
19	38.00 - 36.00	.44001E+01	241.84	.4221E+16	.8391E+16
20	36.00 - 34.00	.58338E+01	236.32	.7147E+16	.1554E+17
21	34.00 - 32.00	.78109E+01	230.90	.1243E+17	.2796E+17
22	32.00 - 30.00	.10905E+02	227.16	.3782E+17	.6579E+17
23	30.00 - 32.00	.10905E+02	227.16	.3782E+17	.1036E+18
24	32.00 - 34.00	.78109E+01	230.90	.1243E+17	.1160E+18
25	34.00 - 36.00	.58338E+01	236.32	.7147E+16	.1232E+18
26	36.00 - 38.00	.44001E+01	241.84	.4221E+16	.1274E+18
27	38.00 - 40.00	.33449E+01	247.33	.2324E+16	.1297E+18
28	40.00 - 42.00	.25598E+01	252.81	.1137E+16	.1309E+18
29	42.00 - 44.00	.19738E+01	258.25	.4689E+15	.1313E+18
30	44.00 - 46.00	.15266E+01	263.74	.1592E+15	.1315E+18
31	46.00 - 48.00	.11849E+01	268.51	.5077E+14	.1315E+18
32	48.00 - 50.00	.92101E+00	270.65	.1760E+14	.1316E+18
33	50.00 - 52.50	.70268E+00	269.38	.8084E+13	.1316E+18
34	52.50 - 55.00	.51399E+00	264.76	.2653E+13	.1316E+18
35	55.00 - 57.50	.37277E+00	257.88	.8378E+12	.1316E+18
36	57.50 - 60.00	.26790E+00	250.98	.2699E+12	.1316E+18
37	60.00 - 62.50	.19122E+00	244.14	.8817E+11	.1316E+18
38	62.50 - 65.00	.13508E+00	237.27	.2757E+11	.1316E+18
39	65.00 - 67.50	.94380E-01	230.40	.8692E+10	.1316E+18
40	67.50 - 70.00	.65242E-01	223.52	.2874E+10	.1316E+18
41	70.00 - 75.00	.39537E-01	215.16	.1649E+10	.1316E+18
42	75.00 - 80.00	.17668E-01	204.39	.3821E+09	.1316E+18
43	80.00 - 90.00	.63409E-02	194.18	.1645E+09	.1316E+18
44	90.00 -100.00	.10857E-02	190.09	.2361E+08	.1316E+18

1.3 Slant path for the Standard Atmosphere
Tangent height 50 km

CO_2

J	Z (KM)	PM (MB)	TM (K)	U (MOLEC/CM2)	SUM(U) (MOLEC/CM2)
1	100.00 - 90.00	.10895E-02	190.07	.9397E+17	.9397E+17
2	90.00 - 80.00	.62661E-02	194.08	.6103E+18	.7043E+18
3	80.00 - 75.00	.17288E-01	204.11	.1044E+19	.1748E+19
4	75.00 - 70.00	.38268E-01	214.66	.2445E+19	.4193E+19
5	70.00 - 67.50	.64193E-01	223.22	.2231E+19	.6423E+19
6	67.50 - 65.00	.92803E-01	230.07	.3362E+19	.9785E+19
7	65.00 - 62.50	.13278E+00	236.93	.5082E+19	.1487E+20
8	62.50 - 60.00	.18813E+00	243.80	.7740E+19	.2261E+20
9	60.00 - 57.50	.26415E+00	250.69	.1200E+20	.3461E+20
10	57.50 - 55.00	.36781E+00	257.59	.1929E+20	.5390E+20
11	55.00 - 52.50	.50884E+00	264.54	.3386E+20	.8776E+20
12	52.50 - 50.00	.72673E+00	269.70	.1143E+21	.2021E+21
13	50.00 - 52.50	.72673E+00	269.70	.1143E+21	.3164E+21
14	52.50 - 55.00	.50884E+00	264.54	.3386E+20	.3502E+21
15	55.00 - 57.50	.36781E+00	257.59	.1929E+20	.3695E+21
16	57.50 - 60.00	.26415E+00	250.69	.1200E+20	.3815E+21
17	60.00 - 62.50	.18813E+00	243.80	.7740E+19	.3892E+21
18	62.50 - 65.00	.13278E+00	236.93	.5082E+19	.3943E+21
19	65.00 - 67.50	.92803E-01	230.07	.3362E+19	.3977E+21
20	67.50 - 70.00	.64193E-01	223.22	.2231E+19	.3999E+21
21	70.00 - 75.00	.38268E-01	214.66	.2445E+19	.4024E+21
22	75.00 - 80.00	.17288E-01	204.11	.1044E+19	.4034E+21
23	80.00 - 90.00	.62661E-02	194.08	.6103E+18	.4040E+21
24	90.00 -100.00	.10895E-02	190.07	.9397E+17	.4041E+21

H_2O

J	Z (KM)	PM (MB)	TM (K)	U (MOLEC/CM2)	SUM(U) (MOLEC/CM2)
1	100.00 - 90.00	.12196E-02	189.37	.1154E+15	.1154E+15
2	90.00 - 80.00	.68477E-02	194.86	.2696E+16	.2811E+16
3	80.00 - 75.00	.17714E-01	204.42	.8453E+16	.1126E+17
4	75.00 - 70.00	.38893E-01	214.91	.2869E+17	.3995E+17
5	70.00 - 67.50	.64409E-01	223.28	.3189E+17	.7184E+17
6	67.50 - 65.00	.92987E-01	230.11	.5310E+17	.1249E+18
7	65.00 - 62.50	.13302E+00	236.97	.8643E+17	.2114E+18
8	62.50 - 60.00	.18829E+00	243.82	.1385E+18	.3499E+18
9	60.00 - 57.50	.26425E+00	250.70	.2201E+18	.5700E+18
10	57.50 - 55.00	.36767E+00	257.58	.3534E+18	.9235E+18
11	55.00 - 52.50	.50864E+00	264.53	.6101E+18	.1534E+19
12	52.50 - 50.00	.72643E+00	269.70	.2020E+19	.3553E+19
13	50.00 - 52.50	.72643E+00	269.70	.2020E+19	.5573E+19
14	52.50 - 55.00	.50864E+00	264.53	.6101E+18	.6183E+19
15	55.00 - 57.50	.36767E+00	257.58	.3534E+18	.6537E+19
16	57.50 - 60.00	.26425E+00	250.70	.2201E+18	.6757E+19
17	60.00 - 62.50	.18829E+00	243.82	.1385E+18	.6895E+19
18	62.50 - 65.00	.13302E+00	236.97	.8643E+17	.6982E+19
19	65.00 - 67.50	.92987E-01	230.11	.5310E+17	.7035E+19
20	67.50 - 70.00	.64409E-01	223.28	.3189E+17	.7067E+19
21	70.00 - 75.00	.38893E-01	214.91	.2869E+17	.7095E+19
22	75.00 - 80.00	.17714E-01	204.42	.8453E+16	.7104E+19
23	80.00 - 90.00	.68477E-02	194.86	.2696E+16	.7107E+19
24	90.00 -100.00	.12196E-02	189.37	.1154E+15	.7107E+19

NO$_2$ Day

J	Z (KM)	PM (MB)	TM (K)	U (MOLEC/CM2)	SUM(U) (MOLEC/CM2)
1	100.00 - 90.00	.10895E-02	190.07	.2848E+08	.2848E+08
2	90.00 - 80.00	.63740E-02	194.22	.2076E+09	.2361E+09
3	80.00 - 75.00	.17705E-01	204.41	.5036E+09	.7397E+09
4	75.00 - 70.00	.39646E-01	215.20	.2279E+10	.3018E+10
5	70.00 - 67.50	.65303E-01	223.54	.4139E+10	.7157E+10
6	67.50 - 65.00	.94485E-01	230.42	.1302E+11	.2017E+11
7	65.00 - 62.50	.13526E+00	237.30	.4335E+11	.6352E+11
8	62.50 - 60.00	.19156E+00	244.17	.1478E+12	.2113E+12
9	60.00 - 57.50	.26855E+00	251.03	.4934E+12	.7047E+12
10	57.50 - 55.00	.37413E+00	257.96	.1743E+13	.2448E+13
11	55.00 - 52.50	.51749E+00	264.91	.6913E+13	.9361E+13
12	52.50 - 50.00	.73781E+00	269.86	.5488E+14	.6424E+14
13	50.00 - 52.50	.73781E+00	269.86	.5488E+14	.1191E+15
14	52.50 - 55.00	.51749E+00	264.91	.6913E+13	.1260E+15
15	55.00 - 57.50	.37413E+00	257.96	.1743E+13	.1278E+15
16	57.50 - 60.00	.26855E+00	251.03	.4934E+12	.1283E+15
17	60.00 - 62.50	.19156E+00	244.17	.1478E+12	.1284E+15
18	62.50 - 65.00	.13526E+00	237.30	.4335E+11	.1285E+15
19	65.00 - 67.50	.94485E-01	230.42	.1302E+11	.1285E+15
20	67.50 - 70.00	.65303E-01	223.54	.4139E+10	.1285E+15
21	70.00 - 75.00	.39646E-01	215.20	.2279E+10	.1285E+15
22	75.00 - 80.00	.17705E-01	204.41	.5036E+09	.1285E+15
23	80.00 - 90.00	.63740E-02	194.22	.2076E+09	.1285E+15
24	90.00 -100.00	.10895E-02	190.07	.2848E+08	.1285E+15

2. Isothermal Atmosphere: T = 250 K

J	z(km)	p(mb)	T(K)
1	8.00	.35651E+03	250.00
2	10.18	.26499E+03	250.00
3	11.31	.22699E+03	250.00
4	12.47	.19399E+03	250.00
5	14.78	.14170E+03	250.00
6	17.09	.10352E+03	250.00
7	19.39	.75652E+02	250.00
8	21.70	.55293E+02	250.00
9	24.00	.40475E+02	250.00
10	26.28	.29717E+02	250.00
11	28.54	.21883E+02	250.00
12	30.78	.16161E+02	250.00
13	33.00	.11970E+02	250.00
14	35.20	.88906E+01	250.00
15	37.37	.66341E+01	250.00
16	39.48	.49852E+01	250.00
17	41.55	.37713E+01	250.00
18	43.57	.28714E+01	250.00
19	45.55	.21996E+01	250.00
20	47.49	.16949E+01	250.00
21	49.38	.13134E+01	250.00
22	51.24	.10229E+01	250.00
23	53.09	.79779E+00	250.00
24	55.41	.58438E+00	250.00
25	57.77	.42525E+00	250.00
26	60.21	.30691E+00	250.00
27	62.70	.21958E+00	250.00
28	65.27	.15567E+00	250.00
29	67.92	.10929E+00	250.00
30	70.64	.75953E-01	250.00
31	73.44	.52209E-01	250.00
32	79.30	.23881E-01	250.00
33	85.45	.10524E-01	250.00
34	98.55	.18359E-02	250.00
35	111.71	.32011E-03	250.00

Trace gas profiles as in section 1

Isothermal Atmosphere: T = 250 K

Tangent height 30 km

CO_2

J	Z (KM)	PM (MB)	TM (K)	U (MOLEC/CM2)	SUM(U) (MOLEC/CM2)
1	111.71 - 98.55	.10868E-02	250.00	.7286E+17	.7286E+17
2	98.55 - 85.45	.62416E-02	250.00	.4583E+18	.5311E+18
3	85.45 - 79.30	.17256E-01	250.00	.7571E+18	.1288E+19
4	79.30 - 73.44	.38168E-01	250.00	.1702E+19	.2991E+19
5	73.44 - 70.64	.64136E-01	250.00	.1492E+19	.4482E+19
6	70.64 - 67.92	.92701E-01	250.00	.2165E+19	.6647E+19
7	67.92 - 65.27	.13260E+00	250.00	.3117E+19	.9764E+19
8	65.27 - 62.70	.18779E+00	250.00	.4451E+19	.1422E+20
9	62.70 - 60.21	.26349E+00	250.00	.6317E+19	.2053E+20
10	60.21 - 57.77	.36643E+00	250.00	.8907E+19	.2944E+20
11	57.77 - 55.41	.50531E+00	250.00	.1250E+20	.4193E+20
12	55.41 - 53.09	.69180E+00	250.00	.1753E+20	.5947E+20
13	53.09 - 51.24	.91101E+00	250.00	.1932E+20	.7879E+20
14	51.24 - 49.38	.11691E+01	250.00	.2603E+20	.1048E+21
15	49.38 - 47.49	.15055E+01	250.00	.3586E+20	.1407E+21
16	47.49 - 45.55	.19493E+01	250.00	.5009E+20	.1908E+21
17	45.55 - 43.57	.25387E+01	250.00	.7099E+20	.2618E+21
18	43.57 - 41.55	.33265E+01	250.00	.1024E+21	.3641E+21
19	41.55 - 39.48	.43868E+01	250.00	.1509E+21	.5150E+21
20	39.48 - 37.37	.58246E+01	250.00	.2292E+21	.7442E+21
21	37.37 - 35.20	.77907E+01	250.00	.3640E+21	.1108E+22
22	35.20 - 33.00	.10492E+02	250.00	.6194E+21	.1728E+22
23	33.00 - 30.00	.15970E+02	250.00	.2955E+22	.4683E+22
24	30.00 - 33.00	.15970E+02	250.00	.2955E+22	.7638E+22
25	33.00 - 35.20	.10492E+02	250.00	.6194E+21	.8258E+22
26	35.20 - 37.37	.77907E+01	250.00	.3640E+21	.8622E+22
27	37.37 - 39.48	.58246E+01	250.00	.2292E+21	.8851E+22
28	39.48 - 41.55	.43868E+01	250.00	.1509E+21	.9002E+22
29	41.55 - 43.57	.33265E+01	250.00	.1024E+21	.9104E+22
30	43.57 - 45.55	.25387E+01	250.00	.7099E+20	.9175E+22
31	45.55 - 47.49	.19493E+01	250.00	.5009E+20	.9225E+22
32	47.49 - 49.38	.15055E+01	250.00	.3586E+20	.9261E+22
33	49.38 - 51.24	.11691E+01	250.00	.2603E+20	.9287E+22
34	51.24 - 53.09	.91101E+00	250.00	.1932E+20	.9306E+22
35	53.09 - 55.41	.69180E+00	250.00	.1753E+20	.9324E+22
36	55.41 - 57.77	.50531E+00	250.00	.1250E+20	.9336E+22
37	57.77 - 60.21	.36643E+00	250.00	.8907E+19	.9345E+22
38	60.21 - 62.70	.26349E+00	250.00	.6317E+19	.9352E+22
39	62.70 - 65.27	.18779E+00	250.00	.4451E+19	.9356E+22
40	65.27 - 67.92	.13260E+00	250.00	.3117E+19	.9359E+22
41	67.92 - 70.64	.92701E-01	250.00	.2165E+19	.9361E+22
42	70.64 - 73.44	.64136E-01	250.00	.1492E+19	.9363E+22
43	73.44 - 79.30	.38168E-01	250.00	.1702E+19	.9365E+22
44	79.30 - 85.45	.17256E-01	250.00	.7571E+18	.9365E+22
45	85.45 - 98.55	.62416E-02	250.00	.4583E+18	.9366E+22
46	98.55 - 111.71	.10868E-02	250.00	.7286E+17	.9366E+22

H_2O

J	Z (KM)	PM (MB)	TM (K)	U (MOLEC/CM2)	SUM(U) (MOLEC/CM2)
1	111.71 - 98.55	.12171E-02	250.00	.8926E+14	.8926E+14
2	98.55 - 85.45	.68235E-02	250.00	.2019E+16	.2108E+16
3	85.45 - 79.30	.17682E-01	250.00	.6125E+16	.8233E+16
4	79.30 - 73.44	.38792E-01	250.00	.1995E+17	.2819E+17
5	73.44 - 70.64	.64351E-01	250.00	.2132E+17	.4951E+17
6	70.64 - 67.92	.92884E-01	250.00	.3418E+17	.8369E+17
7	67.92 - 65.27	.13283E+00	250.00	.5299E+17	.1367E+18
8	65.27 - 62.70	.18795E+00	250.00	.7966E+17	.2163E+18
9	62.70 - 60.21	.26359E+00	250.00	.1159E+18	.3322E+18
10	60.21 - 57.77	.36629E+00	250.00	.1632E+18	.4954E+18
11	57.77 - 55.41	.50512E+00	250.00	.2252E+18	.7206E+18
12	55.41 - 53.09	.69154E+00	250.00	.3107E+18	.1031E+19
13	53.09 - 51.24	.91058E+00	250.00	.3350E+18	.1366E+19
14	51.24 - 49.38	.11687E+01	250.00	.4416E+18	.1808E+19
15	49.38 - 47.49	.15050E+01	250.00	.5975E+18	.2405E+19
16	47.49 - 45.55	.19483E+01	250.00	.8154E+18	.3221E+19
17	45.55 - 43.57	.25374E+01	250.00	.1123E+19	.4344E+19
18	43.57 - 41.55	.33246E+01	250.00	.1573E+19	.5917E+19
19	41.55 - 39.48	.43832E+01	250.00	.2238E+19	.8155E+19
20	39.48 - 37.37	.58195E+01	250.00	.3260E+19	.1142E+20
21	37.37 - 35.20	.77835E+01	250.00	.4956E+19	.1637E+20
22	35.20 - 33.00	.10482E+02	250.00	.8055E+19	.2443E+20
23	33.00 - 30.00	.15946E+02	250.00	.3636E+20	.6079E+20
24	30.00 - 33.00	.15946E+02	250.00	.3636E+20	.9715E+20
25	33.00 - 35.20	.10482E+02	250.00	.8055E+19	.1052E+21
26	35.20 - 37.37	.77835E+01	250.00	.4956E+19	.1102E+21
27	37.37 - 39.48	.58195E+01	250.00	.3260E+19	.1134E+21
28	39.48 - 41.55	.43832E+01	250.00	.2238E+19	.1157E+21
29	41.55 - 43.57	.33246E+01	250.00	.1573E+19	.1172E+21
30	43.57 - 45.55	.25374E+01	250.00	.1123E+19	.1184E+21
31	45.55 - 47.49	.19483E+01	250.00	.8154E+18	.1192E+21
32	47.49 - 49.38	.15050E+01	250.00	.5975E+18	.1198E+21
33	49.38 - 51.24	.11687E+01	250.00	.4416E+18	.1202E+21
34	51.24 - 53.09	.91058E+00	250.00	.3350E+18	.1205E+21
35	53.09 - 55.41	.69154E+00	250.00	.3107E+18	.1209E+21
36	55.41 - 57.77	.50512E+00	250.00	.2252E+18	.1211E+21
37	57.77 - 60.21	.36629E+00	250.00	.1632E+18	.1212E+21
38	60.21 - 62.70	.26359E+00	250.00	.1159E+18	.1214E+21
39	62.70 - 65.27	.18795E+00	250.00	.7966E+17	.1214E+21
40	65.27 - 67.92	.13283E+00	250.00	.5299E+17	.1215E+21
41	67.92 - 70.64	.92884E-01	250.00	.3418E+17	.1215E+21
42	70.64 - 73.44	.64351E-01	250.00	.2132E+17	.1215E+21
43	73.44 - 79.30	.38792E-01	250.00	.1995E+17	.1216E+21
44	79.30 - 85.45	.17682E-01	250.00	.6125E+16	.1216E+21
45	85.45 - 98.55	.68235E-02	250.00	.2019E+16	.1216E+21
46	98.55 -111.71	.12171E-02	250.00	.8926E+14	.1216E+21

NO_2 Day

J	Z (KM)	PM (MB)	TM (K)	U (MOLEC/CM2)	SUM(U) (MOLEC/CM2)
1	111.71 - 98.55	.10868E-02	250.00	.2208E+08	.2208E+08
2	98.55 - 85.45	.63493E-02	250.00	.1558E+09	.1779E+09
3	85.45 - 79.30	.17673E-01	250.00	.3649E+09	.5428E+09
4	79.30 - 73.44	.39545E-01	250.00	.1583E+10	.2126E+10
5	73.44 - 70.64	.65244E-01	250.00	.2764E+10	.4889E+10
6	70.64 - 67.92	.94381E-01	250.00	.8362E+10	.1325E+11
7	67.92 - 65.27	.13507E+00	250.00	.2651E+11	.3976E+11
8	65.27 - 62.70	.19121E+00	250.00	.8464E+11	.1244E+12
9	62.70 - 60.21	.26788E+00	250.00	.2584E+12	.3828E+12
10	60.21 - 57.77	.37272E+00	250.00	.7980E+12	.1181E+13
11	57.77 - 55.41	.51389E+00	250.00	.2509E+13	.3690E+13
12	55.41 - 53.09	.70251E+00	250.00	.7571E+13	.1126E+14
13	53.09 - 51.24	.92083E+00	250.00	.1630E+14	.2756E+14
14	51.24 - 49.38	.11846E+01	250.00	.4647E+14	.7403E+14
15	49.38 - 47.49	.15262E+01	250.00	.1436E+15	.2176E+15
16	47.49 - 45.55	.19731E+01	250.00	.4160E+15	.6336E+15
17	45.55 - 43.57	.25586E+01	250.00	.9884E+15	.1622E+16
18	43.57 - 41.55	.33428E+01	250.00	.1966E+16	.3588E+16
19	41.55 - 39.48	.43961E+01	250.00	.3440E+16	.7028E+16
20	39.48 - 37.37	.58246E+01	250.00	.5487E+16	.1251E+17
21	37.37 - 35.20	.77822E+01	250.00	.8479E+16	.2099E+17
22	35.20 - 33.00	.10460E+02	250.00	.1306E+17	.3406E+17
23	33.00 - 30.00	.15820E+02	250.00	.4807E+17	.8213E+17
24	30.00 - 33.00	.15820E+02	250.00	.4807E+17	.1302E+18
25	33.00 - 35.20	.10460E+02	250.00	.1306E+17	.1433E+18
26	35.20 - 37.37	.77822E+01	250.00	.8479E+16	.1517E+18
27	37.37 - 39.48	.58246E+01	250.00	.5487E+16	.1572E+18
28	39.48 - 41.55	.43961E+01	250.00	.3440E+16	.1607E+18
29	41.55 - 43.57	.33428E+01	250.00	.1966E+16	.1626E+18
30	43.57 - 45.55	.25586E+01	250.00	.9884E+15	.1636E+18
31	45.55 - 47.49	.19731E+01	250.00	.4160E+15	.1640E+18
32	47.49 - 49.38	.15262E+01	250.00	.1436E+15	.1642E+18
33	49.38 - 51.24	.11846E+01	250.00	.4647E+14	.1642E+18
34	51.24 - 53.09	.92083E+00	250.00	.1630E+14	.1642E+18
35	53.09 - 55.41	.70251E+00	250.00	.7571E+13	.1643E+18
36	55.41 - 57.77	.51389E+00	250.00	.2509E+13	.1643E+18
37	57.77 - 60.21	.37272E+00	250.00	.7980E+12	.1643E+18
38	60.21 - 62.70	.26788E+00	250.00	.2584E+12	.1643E+18
39	62.70 - 65.27	.19121E+00	250.00	.8464E+11	.1643E+18
40	65.27 - 67.92	.13507E+00	250.00	.2651E+11	.1643E+18
41	67.92 - 70.64	.94381E-01	250.00	.8362E+10	.1643E+18
42	70.64 - 73.44	.65244E-01	250.00	.2764E+10	.1643E+18
43	73.44 - 79.30	.39545E-01	250.00	.1583E+10	.1643E+18
44	79.30 - 85.45	.17673E-01	250.00	.3649E+09	.1643E+18
45	85.45 - 98.55	.63493E-02	250.00	.1558E+09	.1643E+18
46	98.55 - 111.71	.10868E-02	250.00	.2208E+08	.1643E+18

3. Isothermal Atmosphere: T = 296 K

J	z(km)	p(mb)	T(K)
1	8.00	.35631E+03	296.00
2	10.58	.26499E+03	296.00
3	11.92	.22699E+03	296.00
4	13.29	.19399E+03	296.00
5	16.03	.14170E+03	296.00
6	18.76	.10352E+03	296.00
7	21.50	.75652E+02	296.00
8	24.23	.55293E+02	296.00
9	26.96	.40475E+02	296.00
10	29.66	.29717E+02	296.00
11	32.33	.21883E+02	296.00
12	34.99	.16161E+02	296.00
13	37.62	.11970E+02	296.00
14	40.23	.88906E+01	296.00
15	42.80	.66341E+01	296.00
16	45.31	.49852E+01	296.00
17	47.76	.37715E+01	296.00
18	50.16	.28714E+01	296.00
19	52.51	.21996E+01	296.00
20	54.81	.15949E+01	296.00
21	57.05	.13134E+01	296.00
22	59.26	.10229E+01	296.00
23	61.46	.77779E+00	296.00
24	64.21	.58438E+00	296.00
25	67.02	.42525E+00	296.00
26	69.91	.30691E+00	296.00
27	72.87	.21958E+00	296.00
28	75.92	.15567E+00	296.00
29	79.06	.10929E+00	296.00
30	82.30	.75955E-01	296.00
31	85.63	.52209E-01	296.00
32	92.60	.23881E-01	296.00
33	99.91	.10524E-01	296.00
34	115.49	.13559E-02	296.00
35	131.16	.32011E-03	296.00

Trace gas profiles as in section 1

Isothermal Atmosphere: T = 296 K

Tangent height 30 km

CO_2

J	Z (KM)	PM (MB)	TM (K)	U (MOLEC/CM2)	SUM(U) (MOLEC/CM2)
1	131.16 - 115.49	.10865E-02	296.00	.6584E+17	.6584E+17
2	115.49 - 99.91	.62376E-02	296.00	.4118E+18	.4776E+18
3	99.91 - 92.60	.17252E-01	296.00	.6769E+18	.1155E+19
4	92.60 - 85.63	.38153E-01	296.00	.1516E+19	.2670E+19
5	85.63 - 82.30	.64131E-01	296.00	.1323E+19	.3993E+19
6	82.30 - 79.06	.92696E-01	296.00	.1915E+19	.5908E+19
7	79.06 - 75.92	.13259E+00	296.00	.2748E+19	.8656E+19
8	75.92 - 72.87	.18773E+00	296.00	.3912E+19	.1257E+20
9	72.87 - 69.91	.26346E+00	296.00	.5529E+19	.1810E+20
10	69.91 - 67.02	.36639E+00	296.00	.7763E+19	.2586E+20
11	67.02 - 64.21	.50525E+00	296.00	.1084E+20	.3670E+20
12	64.21 - 61.46	.69171E+00	296.00	.1512E+20	.5181E+20
13	61.46 - 59.26	.91091E+00	296.00	.1656E+20	.6838E+20
14	59.26 - 57.05	.11689E+01	296.00	.2218E+20	.9055E+20
15	57.05 - 54.81	.15053E+01	296.00	.3032E+20	.1209E+21
16	54.81 - 52.51	.19490E+01	296.00	.4197E+20	.1628E+21
17	52.51 - 50.16	.25381E+01	296.00	.5878E+20	.2216E+21
18	50.16 - 47.76	.33254E+01	296.00	.8347E+20	.3051E+21
19	47.76 - 45.31	.43846E+01	296.00	.1205E+21	.4256E+21
20	45.31 - 42.80	.58202E+01	296.00	.1775E+21	.6031E+21
21	42.80 - 40.23	.77804E+01	296.00	.2684E+21	.8715E+21
22	40.23 - 37.62	.10465E+02	296.00	.4165E+21	.1288E+22
23	37.62 - 34.99	.14130E+02	296.00	.6766E+21	.1965E+22
24	34.99 - 32.33	.19181E+02	296.00	.1230E+22	.3194E+22
25	32.33 - 30.00	.26345E+02	296.00	.3667E+22	.6861E+22
26	30.00 - 32.33	.26345E+02	296.00	.3667E+22	.1053E+23
27	32.33 - 34.99	.19181E+02	296.00	.1230E+22	.1176E+23
28	34.99 - 37.62	.14130E+02	296.00	.6766E+21	.1243E+23
29	37.62 - 40.23	.10465E+02	296.00	.4165E+21	.1285E+23
30	40.23 - 42.80	.77804E+01	296.00	.2684E+21	.1312E+23
31	42.80 - 45.31	.58202E+01	296.00	.1775E+21	.1330E+23
32	45.31 - 47.76	.43846E+01	296.00	.1205E+21	.1342E+23
33	47.76 - 50.16	.33254E+01	296.00	.8347E+20	.1350E+23
34	50.16 - 52.51	.25381E+01	296.00	.5878E+20	.1356E+23
35	52.51 - 54.81	.19490E+01	296.00	.4197E+20	.1360E+23
36	54.81 - 57.05	.15053E+01	296.00	.3032E+20	.1363E+23
37	57.05 - 59.26	.11689E+01	296.00	.2218E+20	.1365E+23
38	59.26 - 61.46	.91091E+00	296.00	.1656E+20	.1367E+23
39	61.46 - 64.21	.69171E+00	296.00	.1512E+20	.1369E+23
40	64.21 - 67.02	.50525E+00	296.00	.1084E+20	.1370E+23
41	67.02 - 69.91	.36639E+00	296.00	.7763E+19	.1370E+23
42	69.91 - 72.87	.26346E+00	296.00	.5529E+19	.1371E+23
43	72.87 - 75.92	.18773E+00	296.00	.3912E+19	.1371E+23
44	75.92 - 79.06	.13259E+00	296.00	.2748E+19	.1372E+23
45	79.06 - 82.30	.92696E-01	296.00	.1915E+19	.1372E+23
46	82.30 - 85.63	.64131E-01	296.00	.1323E+19	.1372E+23
47	85.63 - 92.60	.38158E-01	296.00	.1516E+19	.1372E+23
48	92.60 - 99.91	.17252E-01	296.00	.6769E+18	.1372E+23
49	99.91 - 115.49	.62376E-02	296.00	.4118E+18	.1372E+23
50	115.49 - 131.16	.10865E-02	296.00	.6584E+17	.1372E+23

H_2O

J	Z (KM)	PM (MB)	TM (K)	U (MOLEC/CM2)	SUM(U) (MOLEC/CM2)
1	131.16 - 115.49	.12166E-02	296.00	.8063E+14	.8063E+14
2	115.49 - 97.91	.68196E-02	296.00	.1813E+16	.1894E+16
3	97.91 - 92.60	.17678E-01	296.00	.5476E+16	.7370E+16
4	92.60 - 85.63	.38782E-01	296.00	.1776E+17	.2513E+17
5	85.63 - 82.30	.64346E-01	296.00	.1892E+17	.4405E+17
6	82.30 - 79.06	.92877E-01	296.00	.3023E+17	.7428E+17
7	79.06 - 75.92	.13282E+00	296.00	.4672E+17	.1210E+18
8	75.92 - 72.87	.18793E+00	296.00	.7000E+17	.1910E+18
9	72.87 - 69.91	.26556E+00	296.00	.1014E+18	.2924E+18
10	69.91 - 67.02	.36625E+00	296.00	.1423E+18	.4347E+18
11	67.02 - 64.21	.50506E+00	296.00	.1953E+18	.6300E+18
12	64.21 - 61.46	.69145E+00	296.00	.2679E+18	.8979E+18
13	61.46 - 59.26	.91049E+00	296.00	.2872E+18	.1185E+19
14	59.26 - 57.05	.11686E+01	296.00	.3762E+18	.1561E+19
15	57.05 - 54.81	.15048E+01	296.00	.5052E+18	.2066E+19
16	54.81 - 52.51	.19480E+01	296.00	.6831E+18	.2750E+19
17	52.51 - 50.16	.25367E+01	296.00	.9301E+18	.3680E+19
18	50.16 - 47.76	.33235E+01	296.00	.1283E+19	.4962E+19
19	47.76 - 45.31	.43811E+01	296.00	.1788E+19	.6750E+19
20	45.31 - 42.80	.58151E+01	296.00	.2525E+19	.9275E+19
21	42.80 - 40.23	.77732E+01	296.00	.3656E+19	.1293E+20
22	40.23 - 37.62	.10453E+02	296.00	.5419E+19	.1835E+20
23	37.62 - 34.99	.14119E+02	296.00	.8446E+19	.2680E+20
24	34.99 - 32.33	.19165E+02	296.00	.1478E+20	.4158E+20
25	32.33 - 30.00	.26326E+02	296.00	.4234E+20	.8392E+20
26	30.00 - 32.33	.26326E+02	296.00	.4234E+20	.1263E+21
27	32.33 - 34.99	.19165E+02	296.00	.1478E+20	.1410E+21
28	34.99 - 37.62	.14119E+02	296.00	.8446E+19	.1495E+21
29	37.62 - 40.23	.10453E+02	296.00	.5419E+19	.1549E+21
30	40.23 - 42.80	.77732E+01	296.00	.3656E+19	.1586E+21
31	42.80 - 45.31	.58151E+01	296.00	.2525E+19	.1611E+21
32	45.31 - 47.76	.43811E+01	296.00	.1788E+19	.1629E+21
33	47.76 - 50.16	.33235E+01	296.00	.1283E+19	.1642E+21
34	50.16 - 52.51	.25367E+01	296.00	.9301E+18	.1651E+21
35	52.51 - 54.81	.19480E+01	296.00	.6831E+18	.1658E+21
36	54.81 - 57.05	.15048E+01	296.00	.5052E+18	.1663E+21
37	57.05 - 59.26	.11686E+01	296.00	.3762E+18	.1667E+21
38	59.26 - 61.46	.91049E+00	296.00	.2872E+18	.1669E+21
39	61.46 - 64.21	.69145E+00	296.00	.2679E+18	.1672E+21
40	64.21 - 67.02	.50506E+00	296.00	.1953E+18	.1674E+21
41	67.02 - 69.91	.36625E+00	296.00	.1423E+18	.1676E+21
42	69.91 - 72.87	.26556E+00	296.00	.1014E+18	.1677E+21
43	72.87 - 75.92	.18793E+00	296.00	.7000E+17	.1677E+21
44	75.92 - 79.06	.13282E+00	296.00	.4672E+17	.1678E+21
45	79.06 - 82.30	.92877E-01	296.00	.3023E+17	.1678E+21
46	82.30 - 85.63	.64346E-01	296.00	.1892E+17	.1678E+21
47	85.63 - 92.60	.38782E-01	296.00	.1776E+17	.1678E+21
48	92.60 - 97.91	.17678E-01	296.00	.5476E+16	.1678E+21
49	97.91 - 115.49	.68196E-02	296.00	.1813E+16	.1678E+21
50	115.49 - 131.16	.12166E-02	296.00	.8063E+14	.1678E+21

NO_2 Day

J.	Z (KM)	PM (MB)	TM (K)	U (MOLEC/CM2)	SUM(U) (MOLEC/CM2)
1	131.16 -115.49	.10863E-02	296.00	.1995E+08	.1995E+08
2	115.49 - 99.91	.63453E-02	296.00	.1400E+09	.1599E+09
3	99.91 - 92.60	.17669E-01	296.00	.3263E+09	.4862E+09
4	92.60 - 85.63	.39535E-01	296.00	.1409E+10	.1895E+10
5	85.63 - 82.30	.65239E-01	296.00	.2451E+10	.4346E+10
6	82.30 - 79.06	.94373E-01	296.00	.7396E+10	.1174E+11
7	79.06 - 75.92	.13506E+00	296.00	.2337E+11	.3511E+11
8	75.92 - 72.87	.19119E+00	296.00	.7436E+11	.1095E+12
9	72.87 - 69.91	.26785E+00	296.00	.2261E+12	.3356E+12
10	69.91 - 67.02	.37268E+00	296.00	.6953E+12	.1031E+13
11	67.02 - 64.21	.51383E+00	296.00	.2175E+13	.3206E+13
12	64.21 - 61.46	.70241E+00	296.00	.6527E+13	.9733E+13
13	61.46 - 59.26	.92073E+00	296.00	.1397E+14	.2370E+14
14	59.26 - 57.05	.11845E+01	296.00	.3957E+14	.6328E+14
15	57.05 - 54.81	.15260E+01	296.00	.1214E+15	.1847E+15
16	54.81 - 52.51	.19727E+01	296.00	.3683E+15	.5530E+15
17	52.51 - 50.16	.25580E+01	296.00	.8181E+15	.1351E+16
18	50.16 - 47.76	.33416E+01	296.00	.1603E+16	.2954E+16
19	47.76 - 45.31	.43939E+01	296.00	.2746E+16	.5700E+16
20	45.31 - 42.80	.58202E+01	296.00	.4249E+16	.9950E+16
21	42.80 - 40.23	.77720E+01	296.00	.6254E+16	.1620E+17
22	40.23 - 37.62	.10431E+02	296.00	.8794E+16	.2500E+17
23	37.62 - 34.99	.14067E+02	296.00	.1201E+17	.3701E+17
24	34.99 - 32.33	.19062E+02	296.00	.1709E+17	.5410E+17
25	32.33 - 30.00	.26203E+02	296.00	.3784E+17	.9193E+17
26	30.00 - 32.33	.26203E+02	296.00	.3784E+17	.1298E+18
27	32.33 - 34.99	.19062E+02	296.00	.1709E+17	.1469E+18
28	34.99 - 37.62	.14067E+02	296.00	.1201E+17	.1589E+18
29	37.62 - 40.23	.10431E+02	296.00	.8794E+16	.1677E+18
30	40.23 - 42.80	.77720E+01	296.00	.6256E+16	.1739E+18
31	42.80 - 45.31	.58202E+01	296.00	.4249E+16	.1782E+18
32	45.31 - 47.76	.43939E+01	296.00	.2746E+16	.1809E+18
33	47.76 - 50.16	.33416E+01	296.00	.1603E+16	.1825E+18
34	50.16 - 52.51	.25580E+01	296.00	.8181E+15	.1833E+18
35	52.51 - 54.81	.19727E+01	296.00	.3483E+15	.1837E+18
36	54.81 - 57.05	.15260E+01	296.00	.1214E+15	.1838E+18
37	57.05 - 59.26	.11845E+01	296.00	.3957E+14	.1838E+18
38	59.26 - 61.46	.92073E+00	296.00	.1397E+14	.1839E+18
39	61.46 - 64.21	.70241E+00	296.00	.6527E+13	.1839E+18
40	64.21 - 67.02	.51383E+00	296.00	.2175E+13	.1839E+18
41	67.02 - 69.91	.37268E+00	296.00	.6953E+12	.1839E+18
42	69.91 - 72.87	.26785E+00	296.00	.2261E+12	.1839E+18
43	72.87 - 75.92	.19119E+00	296.00	.7436E+11	.1839E+18
44	75.92 - 79.06	.13506E+00	296.00	.2337E+11	.1839E+18
45	79.06 - 82.30	.94373E-01	296.00	.7396E+10	.1839E+18
46	82.30 - 85.63	.65239E-01	296.00	.2451E+10	.1839E+18
47	85.63 - 92.60	.39535E-01	296.00	.1409E+10	.1839E+18
48	92.60 - 99.91	.17669E-01	296.00	.3263E+09	.1839E+18
49	99.91 -115.49	.63453E-02	296.00	.1400E+09	.1839E+18
50	115.49 -131.16	.10863E-02	296.00	.1995E+08	.1839E+18

Appendix B: Quicklook Tables of the Intercomparison

In the following quicklook tables all the results of the ITRA exercises are compared in a special way because the presentation of all plots would be too voluminous. The symbols indicate the worst absolute discrepancy in transmittance/radiance within the whole spectral interval. Discrepancies in the range of lines and gaps between lines are considered separately. Obviously, the agreement between the results of different computer codes has been considerably improved in exercise 2. The significant discrepancies of the isothermal calculations are not clarified up to now.

Remark: The classification of small absolute differences between two plots does not give sufficient information about the agreement in the region of high transmittance or low radiance.

Symbols for classifying the greatest discrepancy in the spectrum:

Transmittance:

– – –:	$-1.0 \leqq$ discr. < -0.1
– –:	$-0.1 \leqq$ discr. < -0.05
–:	$-0.05 \leqq$ discr. < -0.02
±:	$-0.02 \leqq$ discr. $\leqq 0.02$
+:	$0.02 \leqq$ discr. < 0.05
+ +:	$0.05 \leqq$ discr. < 0.1
+ + +:	$0.1 \leqq$ discr. < 1.0
±±:	distinctive discrepancies in both directions

Radiance: (pv = peak value)

– – –:	$-1.0 \cdot pv \leqq$ discr. $< -0.1 \cdot pv$
– –:	$-0.1 \cdot pv \leqq$ discr. $< -0.05 \cdot pv$
–:	$-0.05 \cdot pv \leqq$ discr. $< -0.02 \cdot pv$
±:	$-0.02 \cdot pv \leqq$ discr. $\leqq 0.02 \cdot pv$
+:	$0.02 \cdot pv <$ discr. $< 0.05 \cdot pv$
+ +:	$0.05 \cdot pv \leqq$ discr. $< 0.1 \cdot pv$
+ + +:	$0.1 \cdot pv \leqq$ discr. $< 1.0 \cdot pv$
±±:	distinctive discrepancies in both directions

Case: *Transmittance*		line peaks	gaps
Exercise: *ITRA2*	AFGL – DU	±	±
Wavenumber: *685 – 695cm*$^{-1}$	AFGL – NCAR		
Atmosphere: *US76STD*	AFGL – MIM	±	±
Tangent Height: *10km*	DU – NCAR		
	DU – MIM	±	±
	NCAR – MIM		

Remark: AFGL and MIM calculations of exercise ITRA1

Case: *Transmittance*		line peaks	gaps
Exercise: *ITRA1*	AFGL – DU		
Wavenumber: *685 – 695cm*$^{-1}$	AFGL – NCAR	+ + +	+ +
Atmosphere: *US76STD*	AFGL – MIM	+ +	+
Tangent Height: *30km*	DU – NCAR		
	DU – MIM		
	NCAR – MIM	–	–

Remark: NCAR: greater discrepancies at the edge of the interval

---

Case: *Transmittance*		line peaks	gaps
Exercise: *ITRA2*	AFGL – DU	±	±
Wavenumber: *685 – 695cm*$^{-1}$	AFGL – NCAR	+	±
Atmosphere: *US76STD*	AFGL – MIM	±	±
Tangent Height: *30km*	DU – NCAR	+	±
	DU – MIM	±	±
	NCAR – MIM	–	–

Case: *Transmittance*		line peaks	gaps
Exercise: *ITRA1*	AFGL – DU		
Wavenumber: *685 – 695*cm^{-1}	AFGL – NCAR		
Atmosphere: *ISO296K*	AFGL – MIM	+ + +	±
Tangent Height: *30km*	DU – NCAR		
	DU – MIM		
	NCAR – MIM		

Case: *Transmittance*		line peaks	gaps
Exercise: *ITRA2*	AFGL – DU		
Wavenumber: *685 – 695*cm^{-1}	AFGL – NCAR	±	±
Atmosphere: *ISO296K*	AFGL – MIM	±	±
Tangent Height: *30km*	DU – NCAR		
	DU – MIM		
	NCAR – MIM	±	±

Case: *Transmittance*		line peaks	gaps
Exercise: *ITRA2*	AFGL – DU		
Wavenumber: *685 – 695*cm^{-1}	AFGL – NCAR	+	±
Atmosphere: *ISO250K*	AFGL – MIM		
Tangent Height: *30km*	DU – NCAR		
	DU – MIM		
	NCAR – MIM		

Case: *Transmittance*		line peaks	gaps
Exercise: *ITRA1*	AFGL – DU		
Wavenumber: *685 – 695*cm^{-1}	AFGL – NCAR	±	–
Atmosphere: *US76STD*	AFGL – MIM	±	–
Tangent Height: *50km*	DU – NCAR		
	DU – MIM		
	NCAR – MIM	±	–

Case: *Transmittance*		line peaks	gaps
Exercise: *ITRA2*	AFGL – DU		
Wavenumber: *685 – 695*cm^{-1}	AFGL – NCAR	±	±
Atmosphere: *US76STD*	AFGL – MIM	±	±
Tangent Height: *50km*	DU – NCAR		
	DU – MIM		
	NCAR – MIM	±	–

Case: *Transmittance*		line peaks	gaps
Exercise: *ITRA1*	AFGL – DU		
Wavenumber: *715 – 725*cm^{-1}	AFGL – NCAR		
Atmosphere: *US76STD*	AFGL – MIM		
Tangent Height: *10km*	DU – NCAR		
	DU – MIM		
	NCAR – MIM		+ +

NCAR: border effects

Case: *Transmittance*		line peaks	gaps
Exercise: *ITRA1*	AFGL - DU		
Wavenumber: *715 - 725cm^{-1}*	AFGL - NCAR	+ +	+ +
Atmosphere: *US76STD*	AFGL - MIM	+ +	-
Tangent Height: *30km*	DU - NCAR		
	DU - MIM		
	NCAR - MIM	-	- -

Case: *Transmittance*		line peaks	gaps
Exercise: *ITRA2*	AFGL - DU		
Wavenumber: *715 - 725cm^{-1}*	AFGL - NCAR		
Atmosphere: *US76STD*	AFGL - MIM		
Tangent Height: *30km*	DU - NCAR		
	DU - MIM		
	NCAR - MIM	±	-

Case: *Transmittance*		line peaks	gaps
Exercise: *ITRA1*	AFGL - DU		
Wavenumber: *715 - 725cm^{-1}*	AFGL - NCAR		
Atmosphere: *ISO296K*	AFGL - MIM	+ + +	+ +
Tangent Height: *30km*	DU - NCAR		
	DU - MIM		
	NCAR - MIM		

Case: *Transmittance*		line peaks	gaps
Exercise: *ITRA2*	AFGL - DU		
Wavenumber: *715 - 725cm*$^{-1}$	AFGL - NCAR	±	±
Atmosphere: *ISO296K*	AFGL - MIM	±	±
Tangent Height: *30km*	DU - NCAR		
	DU - MIM		
	NCAR - MIM	±	–

Case: *Transmittance*		line peaks	gaps
Exercise: *ITRA2*	AFGL - DU		
Wavenumber: *715 - 725cm*$^{-1}$	AFGL - NCAR	+	+
Atmosphere: *ISO250K*	AFGL - MIM		
Tangent Height: *30km*	DU - NCAR		
	DU - MIM		
	NCAR - MIM		

Case: *Transmittance*		line peaks	gaps
Exercise: *ITRA1*	AFGL - DU		
Wavenumber: *715 - 725cm*$^{-1}$	AFGL - NCAR	±	+
Atmosphere: *US76STD*	AFGL - MIM	±	±
Tangent Height: *50km*	DU - NCAR		
	DU - MIM		
	NCAR - MIM	±	+

Case: *Transmittance*		line peaks	gaps
Exercise: *ITRA2*	AFGL - DU		
Wavenumber: *715 - 725cm*$^{-1}$	AFGL - NCAR		
Atmosphere: *US76STD*	AFGL - MIM		
Tangent Height: *50km*	DU - NCAR		
	DU - MIM		
	NCAR - MIM	±	±

Case: *Transmittance*		line peaks	gaps
Exercise: *ITRA1*	AFGL - DU		
Wavenumber: *732 - 764cm*$^{-1}$	AFGL - NCAR		
Atmosphere: *US76STD*	AFGL - MIM	±	−
Tangent Height: *30km*	DU - NCAR		
	DU - MIM		
	NCAR - MIM		

Case: *Transmittance*		line peaks	gaps
Exercise: *ITRA2*	AFGL - DU		
Wavenumber: *732 - 764cm*$^{-1}$	AFGL - NCAR		
Atmosphere: *US76STD*	AFGL - MIM		
Tangent Height: *30km*	DU - NCAR		
	DU - MIM		
	NCAR - MIM	±	−

Case: *Transmittance*		line peaks	gaps
Exercise: *ITRA1*	AFGL - DU		
Wavenumber: *732 - 764cm^{-1}*	AFGL - NCAR		
Atmosphere: *ISO296K*	AFGL - MIM	+ +	+ +
Tangent Height: *30km*	DU - NCAR		
	DU - MIM		
	NCAR - MIM		

Case: *Transmittance*		line peaks	gaps
Exercise: *ITRA2*	AFGL - DU		
Wavenumber: *732 - 764cm^{-1}*	AFGL - NCAR		
Atmosphere: *ISO296K*	AFGL - MIM		
Tangent Height: *30km*	DU - NCAR		
	DU - MIM		
	NCAR - MIM	+	+

Case: *Transmittance*		line peaks	gaps
Exercise: *ITRA1*	AFGL - DU		
Wavenumber: *732 - 764cm^{-1}*	AFGL - NCAR		
Atmosphere: *US76STD*	AFGL - MIM	±	±
Tangent Height: *50km*	DU - NCAR		
	DU - MIM		
	NCAR - MIM		

Case: *Transmittance*		line peaks	gaps
Exercise: *ITRA2*	AFGL – DU		
Wavenumber: *732 – 764cm^{-1}*	AFGL – NCAR		
Atmosphere: *US76STD*	AFGL – MIM		
Tangent Height: *50km*	DU – NCAR		
	DU – MIM		
	NCAR – MIM	±	–

Case: *Transmittance*		line peaks	gaps
Exercise: *ITRA1*	AFGL – DU	– – –	– – –
Wavenumber: *1600 – 1610cm^{-1}*	AFGL – NCAR	– – –	– – –
Atmosphere: *US76STD*	AFGL – MIM	– – –	– – –
Tangent Height: *10km*	DU – NCAR	– – –	– – –
	DU – MIM	+ + +	+ + +
	NCAR – MIM	+ + +	+ + +

See Fig. 5 and discussion in section 4.4

Case: *Transmittance*		line peaks	gaps
Exercise: *ITRA1*	AFGL – DU	±	±
Wavenumber: *1600 – 1610cm^{-1}*	AFGL – NCAR	±	–
Atmosphere: *US76STD*	AFGL – MIM	±	±
Tangent Height: *30km*	DU – NCAR	±	–
	DU – MIM	±	±
	NCAR – MIM	±	+

Case: *Transmittance*		line peaks	gaps
Exercise: *ITRA2*	AFGL - DU	±	±
Wavenumber: *1600 - 1610cm*$^{-1}$	AFGL - NCAR		
Atmosphere: *US76STD*	AFGL - MIM	±	±
Tangent Height: *30km*	DU - NCAR		
	DU - MIM	±	±
	NCAR - MIM		

Case: *Transmittance*		line peaks	gaps
Exercise: *ITRA1*	AFGL - DU		
Wavenumber: *1600 - 1610cm*$^{-1}$	AFGL - NCAR		
Atmosphere: *US76STD*	AFGL - MIM		
Tangent Height: *50km*	DU - NCAR	±	- -
	DU - MIM	±	±
	NCAR - MIM	±	+ +

Case: *Transmittance*		line peaks	gaps
Exercise: *ITRA2*	AFGL - DU		
Wavenumber: *1600 - 1610cm*$^{-1}$	AFGL - NCAR		
Atmosphere: *US76STD*	AFGL - MIM	±	±
Tangent Height: *50km*	DU - NCAR		
	DU - MIM		
	NCAR - MIM		

Case: *Radiance*		rad.	peaks	gaps
Exercise: *ITRA1*	AFGL - DU			
Wavenumber: *685 - 695cm*$^{-1}$	AFGL - NCAR	–		±
Atmosphere: *US76STD*	AFGL - MIM	–		±
Tangent Height: *10km*	DU - NCAR			
	DU - MIM			
	NCAR - MIM	±		±

Case: *Radiance*		rad.	peaks	gaps
Exercise: *ITRA2*	AFGL - DU			
Wavenumber: *685 - 695cm*$^{-1}$	AFGL - NCAR	±		±
Atmosphere: *US76STD*	AFGL - MIM			
Tangent Height: *10km*	DU - NCAR			
	DU - MIM			
	NCAR - MIM			

Case: *Radiance*		rad.	peaks	gaps
Exercise: *ITRA1*	AFGL - DU			
Wavenumber: *685 - 695cm*$^{-1}$	AFGL - NCAR	–		– –
Atmosphere: *US76STD*	AFGL - MIM	±		– –
Tangent Height: *30km*	DU - NCAR			
	DU - MIM			
	NCAR - MIM	+		+

Case: *Radiance*		rad.	peaks	gaps
Exercise: *ITRA2*	AFGL – DU	±		±
Wavenumber: *685 – 695*cm^{-1}	AFGL – NCAR	–		–
Atmosphere: *US76STD*	AFGL – MIM	±		±
Tangent Height: *30km*	DU – NCAR	±		–
	DU – MIM	±		±
	NCAR – MIM	±		+

Case: *Radiance*		rad.	peaks	gaps
Exercise: *ITRA1*	AFGL – DU			
Wavenumber: *685 – 695*cm^{-1}	AFGL – NCAR			
Atmosphere: *ISO296K*	AFGL – MIM	±		– – –
Tangent Height: *10km*	DU – NCAR			
	DU – MIM			
	NCAR – MIM			

Case: *Radiance*		rad.	peaks	gaps
Exercise: *ITRA2*	AFGL – DU			
Wavenumber: *685 – 695*cm^{-1}	AFGL – NCAR	±		±
Atmosphere: *ISO296K*	AFGL – MIM	±		±
Tangent Height: *30km*	DU – NCAR			
	DU – MIM			
	NCAR – MIM	±		±

Case: *Radiance*		rad.	peaks	gaps
Exercise *ITRA2*	AFGL – DU			
Wavenumber: *685 – 695cm*$^{-1}$	AFGL – NCAR	±		–
Atmosphere: *ISO250K*	AFGL – MIM			
Tangent Height: *30km*	DU – NCAR			
	DU – MIM			
	NCAR – MIM			

Case: *Radiance*		rad.	peaks	gaps
Exercise: *ITRA1*	AFGL – DU			
Wavenumber: *685 – 695cm*$^{-1}$	AFGL – NCAR	–		±
Atmosphere: *US76STD*	AFGL – MIM	±		±
Tangent Height: *50km*	DU – NCAR			
	DU – MIM			
	NCAR – MIM	+		±

Case: *Radiance*		rad.	peaks	gaps
Exercise: *ITRA2*	AFGL – DU			
Wavenumber: *685 – 695cm*$^{-1}$	AFGL – NCAR	–		±
Atmosphere: *US76STD*	AFGL – MIM	±		±
Tangent Height: *50km*	DU – NCAR			
	DU – MIM			
	NCAR – MIM	±		±

Case: *Radiance*

Exercise: *ITRA1*
Wavenumber: *715 – 725cm*$^{-1}$
Atmosphere: *US76STD*
Tangent Height: *10km*

	rad.	peaks	gaps
AFGL – DU			
AFGL – NCAR			
AFGL – MIM			
DU – NCAR			
DU – MIM			
NCAR – MIM	+		+

Case: *Radiance*

Exercise: *ITRA1*
Wavenumber: *715 – 725cm*$^{-1}$
Atmosphere: *US76STD*
Tangent Height: *30km*

	rad.	peaks	gaps
AFGL – DU			
AFGL – NCAR	–		±
AFGL – MIM	+		–
DU – NCAR			
DU – MIM			
NCAR – MIM	+		±

Case: *Radiance*

Exercise: *ITRA2*
Wavenumber: *715 – 725cm*$^{-1}$
Atmosphere: *US76STD*
Tangent Height: *30km*

	rad.	peaks	gaps
AFGL – DU			
AFGL – NCAR			
AFGL – MIM			
DU – NCAR			
DU – MIM			
NCAR – MIM	+ +		±

Case: *Radiance*		rad.	peaks	gaps
Exercise: *ITRA1*	AFGL – DU	±		±
Wavenumber: *715 – 725cm*$^{-1}$	AFGL – NCAR			
Atmosphere: *ISO296K*	AFGL – MIM	– –		– – –
Tangent Height: *30km*	DU – NCAR			
	DU – MIM			
	NCAR – MIM			

Case: *Radiance*		rad.	peaks	gaps
Exercise: *ITRA2*	AFGL – DU			
Wavenumber: *715 – 725cm*$^{-1}$	AFGL – NCAR	±		–
Atmosphere: *ISO296K*	AFGL – MIM	±		±
Tangent Height: *30km*	DU – NCAR			
	DU – MIM			
	NCAR – MIM	+		±

Case: *Radiance*		rad.	peaks	gaps
Exercise: *ITRA2*	AFGL – DU			
Wavenumber: *715 – 725cm*$^{-1}$	AFGL – NCAR	+		±
Atmosphere: *ISO250K*	AFGL – MIM			
Tangent Height: *30km*	DU – NCAR			
	DU – MIM			
	NCAR – MIM			

Case: *Radiance*		rad.	peaks	gaps
Exercise: *ITRA1*	AFGL – DU			
Wavenumber: *715 – 725cm*$^{-1}$	AFGL – NCAR	– –		±
Atmosphere: *US76STD*	AFGL – MIM	+		±
Tangent Height: *50km*	DU – NCAR			
	DU – MIM			
	NCAR – MIM	+ +		±

Case: *Radiance*		rad.	peaks	gaps
Exercise: *ITRA2*	AFGL – DU			
Wavenumber: *715 – 725cm*$^{-1}$	AFGL – NCAR			
Atmosphere: *US76STD*	AFGL – MIM			
Tangent Height: *50km*	DU – NCAR			
	DU – MIM			
	NCAR – MIM	+		±

Case: *Radiance*		rad.	peaks	gaps
Exercise: *ITRA1*	AFGL – DU			
Wavenumber: *732 – 764cm*$^{-1}$	AFGL – NCAR			
Atmosphere: *US76STD*	AFGL – MIM	±		–
Tangent Height: *10km*	DU – NCAR			
	DU – MIM			
	NCAR – MIM			

Case: *Radiance*		rad.	peaks	gaps
Exercise: *ITRA1*	AFGL – DU			
Wavenumber: *732 – 764*cm^{-1}	AFGL – NCAR			
Atmosphere: *US76STD*	AFGL – MIM	+		–
Tangent Height: *30km*	DU – NCAR			
	DU – MIM			
	NCAR – MIM			

Case: *Radiance*		rad.	peaks	gaps
Exercise: *ITRA2*	AFGL – DU			
Wavenumber: *732 – 764*cm^{-1}	AFGL – NCAR			
Atmosphere: *US76STD*	AFGL – MIM			
Tangent Height: *30km*	DU – NCAR			
	DU – MIM			
	NCAR – MIM	(+ + +)		±

Remark about NCAR results: The normalization of the second part of the interval is different. The first part of the interval fits quite well to the MIM – plot.

Case: *Radiance*		rad.	peaks	gaps
Exercise: *ITRA1*	AFGL – DU			
Wavenumber: *732 – 764*cm^{-1}	AFGL – NCAR			
Atmosphere: *ISO296K*	AFGL – MIM	±		–
Tangent Height: *30km*	DU – NCAR			
	DU – MIM			
	NCAR – MIM			

Case: *Radiance*		rad.	peaks	gaps
Exercise: *ITRA2*	AFGL - DU			
Wavenumber: *732 - 764cm^{-1}*	AFGL - NCAR			
Atmosphere: *ISO296K*	AFGL - MIM			
Tangent Height: *30km*	DU - NCAR			
	DU - MIM			
	NCAR - MIM	(+ +)		±

NCAR: see above

Case: *Radiance*		rad.	peaks	gaps
Exercise: *ITRA1*	AFGL - DU			
Wavenumber: *732 - 764cm^{-1}*	AFGL - NCAR			
Atmosphere: *US76STD*	AFGL - MIM	+		±
Tangent Height: *50km*	DU - NCAR			
	DU - MIM			
	NCAR - MIM			

Case: *Radiance*		rad.	peaks	gaps
Exercise: *ITRA2*	AFGL - DU			
Wavenumber: *732 - 764cm^{-1}*	AFGL - NCAR			
Atmosphere: *US76STD*	AFGL - MIM			
Tangent Height: *50km*	DU - NCAR			
	DU - MIM			
	NCAR - MIM	(- - -)		±

NCAR: see above

Case: *Radiance*		rad.	peaks	gaps
Exercise: *ITRA1*	AFGL - DU			
Wavenumber: *1600 - 1610cm⁻¹*	AFGL - NCAR	± ± ±		+ + +
Atmosphere: *US76STD*	AFGL - MIM	+		+ + +
Tangent Height: *10km*	DU - NCAR			
	DU - MIM			
	NCAR - MIM	± ± ±		− − −

See Fig. 5 and discussion in section 4.4

Case: *Radiance*		rad.	peaks	gaps
Exercise: *ITRA1*	AFGL - DU	+		±
Wavenumber: *1600 - 1610cm⁻¹*	AFGL - NCAR	−		±
Atmosphere: *US76STD*	AFGL - MIM	+		±
Tangent Height: *30km*	DU - NCAR	− −		±
	DU - MIM	+		±
	NCAR - MIM	+ +		±

Case: *Radiance*		rad.	peaks	gaps
Exercise: *ITRA2*	AFGL - DU	±		±
Wavenumber: *1600 - 1610cm⁻¹*	AFGL - NCAR			
Atmosphere: *US76STD*	AFGL - MIM	±		±
Tangent Height: *30km*	DU - NCAR			
	DU - MIM	±		±
	NCAR - MIM			

Case: *Radiance*		rad.	peaks	gaps
Exercise: *ITRA1*	AFGL – DU			
Wavenumber: *1600 – 1610cm*$^{-1}$	AFGL – NCAR			
Atmosphere: *US76STD*	AFGL – MIM			
Tangent Height: *50km*	DU – NCAR			
	DU – MIM			
	NCAR – MIM	± ± ±		±

Case: *Radiance*		rad.	peaks	gaps
Exercise: *ITRA2*	AFGL – DU			
Wavenumber: *1600 – 1610cm*$^{-1}$	AFGL – NCAR			
Atmosphere: *US76STD*	AFGL – MIM	–		±
Tangent Height: *50km*	DU – NCAR			
	DU – MIM			
	NCAR – MIM			

Appendix C: Additional Plots

Fig. C1, typical ITRA 2 result, CO_2, 715 - 725 cm^{-1},
radiance, z_{min} = 30 km, NCAR

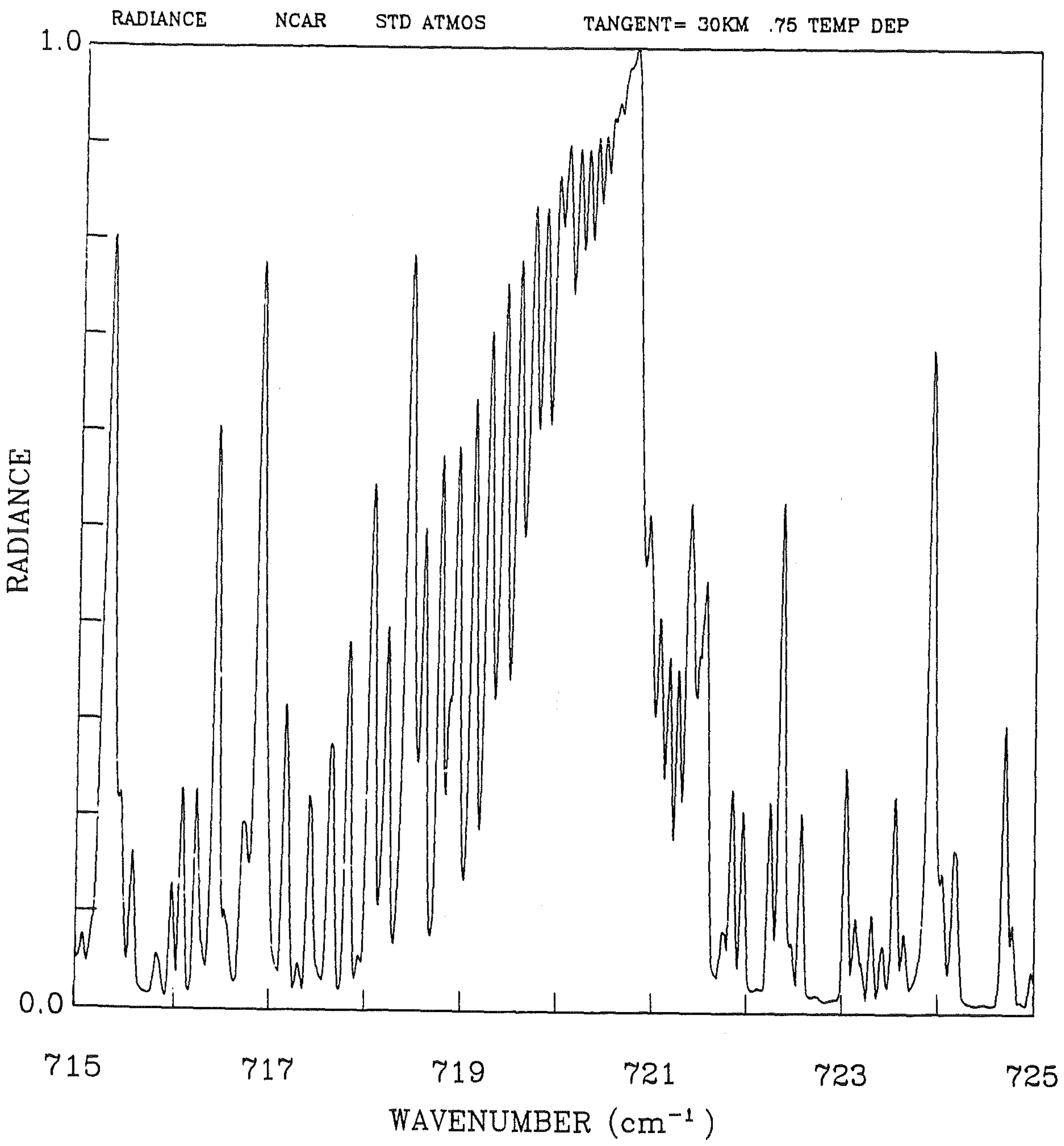

Fig. C2, typical ITRA1 result, CO_2, 732 - 764 cm^{-1}, US76Std radiance, z_{min} = 30 km, AFGL

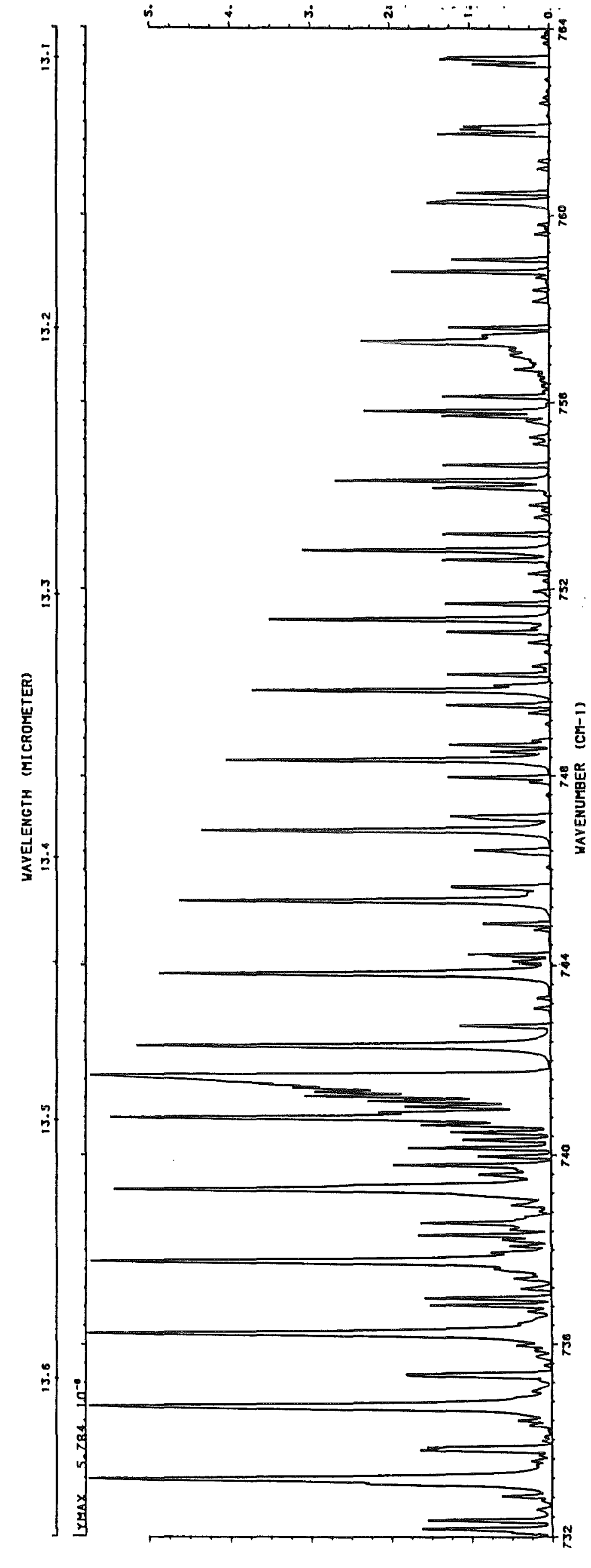

Appendix D: Brief Descriptions of the Line – By – Line Computer Codes

In order to inform the reader about the main differences of the line – by – line computer codes brief descriptions of these codes are given below:

1. Air Force Geophysics Lab/FASCOD2

(S.A. Clough, G.P. Anderson, F.X. Kneizys, E.P. Shettle)

FASCOD2 (Fast Atmospheric Signature Code) is a computer code for the accelerated line – by – line calculation of spectral transmittance and radiance for both atmospheric and laboratory conditions (Clough et al. 1987, Clough et al. 1986, Clough et al. 1981, and Smith et al. 1978). The program is applicable to spectral regions from the microwave to the near ultraviolet and uses a Voigt line shape with a bound of 25 cm^{-1}. Line wing contributions more than 25 cm^{-1} from line center are contained in precalculated continua.

The program assumes a spherically layered atmoshere and is applicable to any slant path geometry, fully accomodating spherical refractive geometry within the layering structure; that is, integrated column densities, ranges, tangent heights, and other geometric factors are derived by integrating along the line of sight using either exponential (pressure, densities) or linear (temperature) interpolation between layer boundaries. This permits layer selection to reflect the actual thermal and/or pressure gradients rather than geometric considerations, generally eliminating the need for special sub – layering at tangent heights.

The FASCOD2 line – by – line algorithm determines the mean Voigt line width for each layer and optimally synthesizes the correct line shape based on 4 Lorentz fitting functions, plus the continua. The first three functions represent the line behavior within 4, 16, and 64 halfwidths while the 4th contains the line contributions out to 25 cm^{-1}. Their rapid convolution with spectroscopic line data provides factors of 10 advantage in speed over conventional line – by – line codes. The full Voigt line shape formulation requires two additional terms, each of which is optimally interpolated from prestored coefficients; ultimately the Voigt profile requires only 20% more computational time than the already efficient FASCOD2 Lorentz algorithm.

The continua are, in part, predicated on prior selection of modifying χ – factors to account for non – Lorentzian line shapes for CO_2 and self and foreign broadened water vapor.

For CO_2, this χ – factor is sub – Lorentzian at all spectral distances from line center, and is synthesized in FASCOD2 by both the near (less than 25 cm^{-1}) line shape contribution functions and the precalculated CO_2 continuum.

The χ - factors for H_2O (one for self and one for foreign broadening) do not behave like CO_2. While near line center they are approximately unity, both χ - factors become super - Lorentzian near 25 cm^{-1} from line center, ultimately returning to sub - Lorentzian values thereafter. Both the super and the sub - Lorentzian behaviors are contained in the H_2O continua calculations, leading to strong spectral dependencies. At 1600 cm^{-1} the combined H_2O continua provide significantly larger attenuation than that calculated by assuming Lorentz line shape (see Fig. 5). However, at 1000 cm^{-1} the H_2O continua values are substantially smaller than those arising from a strict Lorentz line shape, potentially yielding less calculated absorption. [See Clough, et al.,(1987)]

Full spectral resolution is maintained at all pressure levels, dependent only upon the pressure levels and temperature dependence of the Voigt line characteristics. The exponent which describes the temperature dependence of the collisional broadened halfwidths is internally defined with typical ranges between 0.5 and 1.0. ITRA2 requested 0.75 for CO_2 and 0.5 for H_2O and NO_2.

References:

Clough, S.A., F.X. Kneizys, L.S. Rothman, G.P. Anderson, and E.P. Shettle, 1987 (in press): Current Issues in Infrared Atmospheric Transparency, Proceedings of the Capri Workshop on Atmospheric Transparency, Sept 1986, Capri, Italy.

Clough, S.A., F.X. Kneizys, E.P. Shettle, and G.P. Anderson, 1986: Atmospheric Radiance and Transmittance: FASCOD2, Proceedings of the Sixth Conference on Atmospheric Radiation, May 1986, Williamsburg, VA.

Clough, S.A., F.X. Kneizys, L.S. Rothman, and W.O. Gallery, 1981: Atmospheric Spectral Transmittance and Radiance: FASCOD 1B, Proceedings of SPIE, 277, Atm. Transm.

Smith, H.J.P., D.J. Dube, M.E. Gardner, S.A. Clough, F.X. Kneizys, and L.S. Rothman, 1978: FASCOD - Fast Atmosphere Signature Code (Spectral Transmittance and Radiance), AFGL - TR - 78 - 0081.

2. NCAR (M.T. Coffey and W.G. Mankin)

The Fourier transform method (Mankin, 1979) for calculating the transmittance of inhomogeneous atmospheres is a very efficient method when large numbers of spectral lines are required. The method computes the time consuming convolution of the line shape at each spectral line by transforming into Fourier space. The line shape is in general produced by a combination of Doppler and pressure broadening. The resulting Voigt profile is laborious to compute in spectral space, being a convolution of a Gaussian and a Lorentzian profile; on the other hand the Fourier transform of the Voigt profile requires only one exponential calculation. Shifting the profile to line center in spectral space requires multiplication by a complex exponential in the Fourier conjugate space.

A great advantage of the method is that the computation time is almost independent of the number of absorption lines in the calculation; most of the computation time is taken in the Fast Fourier Transform.

A major simplifying assumption is that all lines have the same halfwidth and shape; for many cases this is an adequate assumption. In the calculation presented in this report each line shape was represented by the linear combination of two constant shapes which even better approximates the actual shape. The influence of the wings of each line are included at all points in the spectral range of calculation, there is no arbitrary cutoff of the influence of the wings. Care must be taken to calculate a range sufficiently large with respect to the wavelengths of interest so that the influence of the wings of adjacent regions may be included. The NCAR calculation of the water vapor absorption in the 1600 – 1610 cm^{-1} region (Figure 5) shows a case where the contribution of the wings outside the 1600 – 1610 cm^{-1} region was not included.

A second limiting assumption is that layers in the calculation are isothermal; this is not a severe restriction in the stratosphere or with large numbers of layers in the present calculations. Mixing ratios and pressure are allowed to vary continuously in a layer. This is a major departure from homogenous layer models and allows for the use of fewer, thicker layers thus further reducing computation time.

We assume a plane parallel atmosphere without refraction.

Reference:

W.G. Mankin, Fourier transform method for calculating the transmittance of inhomogeneous atmospheres, Applied Optics, 18, 3426, 1979.

3. University of Denver (A. Goldman)

The University of Denver computer program used for this study is a "direct" (in the wavenumber space) line by line – layer by layer calculation, optimised to run on the Cray computers system at NCAR. It is based, in part, on the line by line program initiated by Kyle (1969), which went through several modifications, upgrades, and optimisations. The program is very flexible and allows increased accuracy by interpolating from refined stepsizes of the basic parameters such as the number of atmospheric layers (up to 64, but only 32 used here) and the variable mesh points for the line shape (usually 0.001 cm^{-1}, but can be adjusted to larger or smaller values, depending on the problem and the pressure range). The program can handle different wings intervals, half-widths, and several variations on the Voigt line shape (the only one used for present study). Full account is taken of atmospheric refraction and various options are available for the atmospheric pressure, temperature, and trace gases mixing ratio profiles. Continuum is included in this program as several sets of "gray" coefficients (but none used here).

Over the years, this program has been compared with several other line by line codes, and excellent agreement was achieved: 4 to 5 digits on spectral transmittance and radiance when complete details of atmospheric and spectroscopic parameters are identical.

Reference:

T. G. Kyle, "Calculations of Atmospheric Transmittance from 1.7 to 20 μ", J. Quant. Spectrosc. Radiat. Transfer 9, 1477 – 1488, 1969.

4. University of Munich (MIM, H. Fischer et al.)

The calculation of absorber amount and mean values of pressure and temperature of atmospheric layers is done by an iterative algorithm. Each layer is divided into eight sublayers, which contain approximately the same absorber amount. Using this method interpolation and averaging errors are kept small. Atmospheric refraction is taken into account.

The algorithm for calculating the Voigt profile is based on the proposal by *Drayson* (1976). The line wings can be modified with a χ - factor. In case of CO_2 sub - Lorentzian line wings are assumed while for all other gases Lorentzian line wings are used generally.

The line - by - line code is characterized by the consideration of all available lines within and outside the given spectral interval which are contributing to the absorption coefficient at any mesh point within the given spectral interval: The selection of the contributing lines is done with a special altitude - dependent criterion. The wings of the lines outside the given spectral interval are superimposed to form a quasi - continuum (Redemann, 1984)

The temperature dependence of the line intensity includes the temperature dependence of the vibrational partition functions as given by *Young* (1976).

The exponent n for the temperature dependance of the half width is variable. In case of CO_2 n is 0.75, in case of H_2O 0.5 and in case of NO_2 0.967.

The MIM line - by - line code does not consider line interference up to now.

Variable frequency mesh points are used, beginning with $\Delta v = 5 \cdot 10^{-4}$ cm^{-1} near the line center, increasing with increasing distance up to a constant value of 0.01 cm^{-1} dependent on the spacing of the lines of the absorbing species. The frequency integration is done according to the trapezoidal rule.

The first priority of the MIM line - by - line code is to accomplish high accuracy while saving computer time has only the second priority. Therefore, this code is more appropriate for the investigation of special problems or the processing of single measurements than for operational use.

References:

L.G. Young, Compilation of Stratospheric Trace Gas Spectral Parameters, Report AFCRL - TR - 76 - 0033, 1976

S.R. Drayson, Rapid Computation of the Voigt profile, J. Quant. Spectrosc. Radiat. Transfer, 16, 611 - 614, 1976

E. Redemann, Ein FORTRAN - Rechenprogramm zur Berechnung der atmosphärischen Transmission und Strahldichte; Universität München - Meteorologisches Institut, 1984, unpublished

Appendix E: Address List of Limb – Subgroup Participants

Ms. G.P. Anderson
Infrared Physics Branch
Optical Physics Division
Air Force Geophysics Laboratory
Hanscom Air Force Base, MA 01731
USA

Mr. Thomas v. Clarmann
Institute of Meteorology and Climate Research
Kernforschungszentrum Karlsruhe
Postfach 3640
D – 7500 Karlsruhe 1
Federal Republic of Germany

Dr. Shepard A. Clough
Infrared Physics Branch
Optical Physics Division
Air Force Geophysics Laboratory
Hanscom Air Force Base, MA 01731
USA

Dr. M.T. Coffey
NCAR
P. O. Box 3000
Boulder, CO 80307
USA

Dr. Herbert Fischer
Institute of Meteorology and Climate Research
Kernforschungszentrum Karlsruhe
Postfach 3640
D – 7500 Karlsruhe 1
Federal Republic of Germany

Former address:
Meteorologisches Institut
Universität München
Theresienstraße 37
D – 8000 München 2
Federal Republic of Germany

Dr. A. Goldman
University of Denver
Department of Physics
Denver, CO 80208
USA

Dr. Larry L. Gordley
Mail Stop 401A
NASA Langley Research Center
Hampton, VA 23665 - 5225
USA

Dr. F.X. Kneizys
Infrared Physics Branch
Optical Physics Division
Air Force Geophysics Laboratory
Hanscom Air Force Base, MA 01713
USA

Dr. Virgil Kunde
NASA/Goddard Space Flight Center
Code 693
Greenbelt, MD 20771
USA

Dr. L. Rothman
Air Force Geophysics Laboratory
Hanscom Air Force Base
Bedford, MA 01731
USA

Address of the ITRA - chairman:

Dr. A. Chedin
Laboratoire De Meteorologie Dynamique Du C.N.R.S.
Ecole Polytechnique
F - 91128 Palaiseau Cedex
France